A SEDIMENT COMPOSITE FINGERPRINTING TOOL: A FIELD-BASED QUANTIFICATION METHOD OF THE SEDIMENT ORIGIN WITHIN A WATER ENVIRONMENT- A PILOT STUDY

by

Thanos Papanicolaou, Ozan Abaci, and Ranjani Theregowda

Sponsored by
the Iowa Department of Natural Resources

IIHR Technical Report #455

IIHR-Hydroscience & Engineering
College of Engineering
The University of Iowa
Iowa City, Iowa 52242

June 2006

A SEDIMENT COMPOSITE FINGERPRINTING TOOL: A FIELD-BASED QUANTIFICATION METHOD OF THE SEDIMENT ORIGIN WITHIN A WATER ENVIRONMENT- A PILOT STUDY

FINAL REPORT

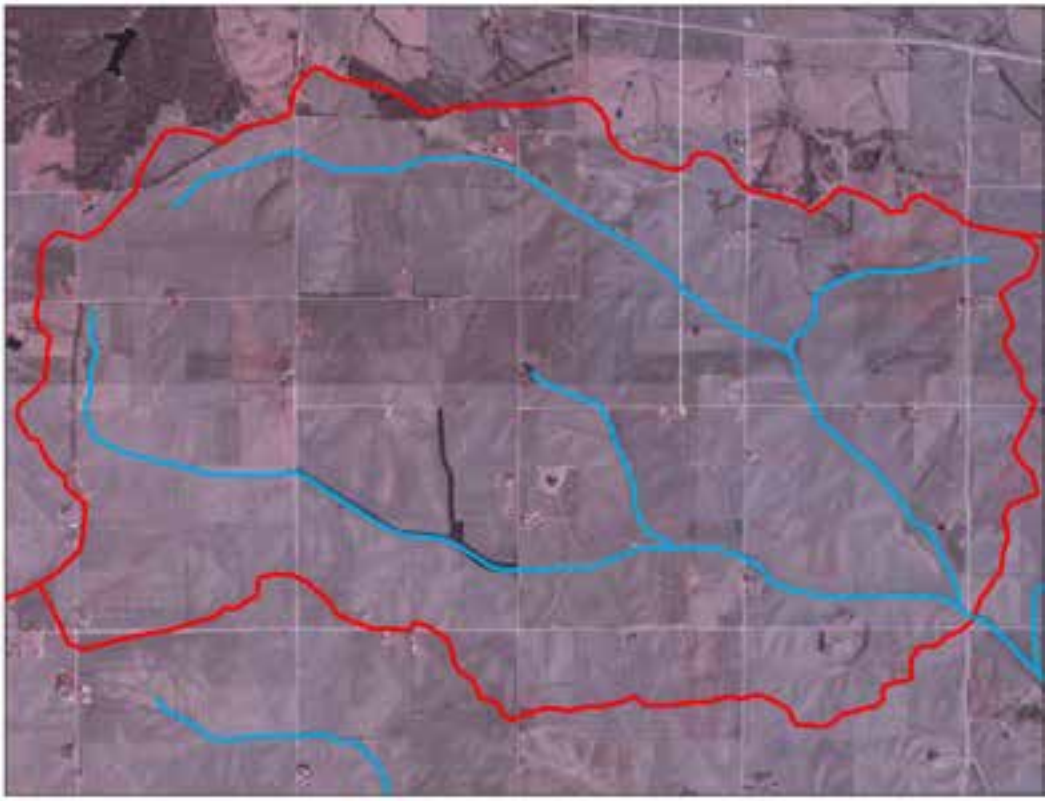

Submitted to:
Dr. Mary Skopec
Iowa Department of Natural Resources
109 Trowbridge Hall
Iowa City, IA 52242-1319

About the IIHR- Hydroscience & Engineering

IIHR, a unit of The University of Iowa's College of Engineering, is one of the nation's premier and oldest fluids research and engineering laboratories. Situated on the Iowa River in Iowa City, Iowa, IIHR seeks to educate students and to conduct research in the broad fields of hydraulics and fluid mechanics.

Disclaimer Notice

The contents of this report reflect the views of the authors, who are responsible for the facts and the accuracy of the information presented herein. The opinions, findings and conclusions expressed in this publication are those of the authors and not necessarily those of the sponsors.

The sponsors assume no liability for the contents or use of the information contained in this document. This report does not constitute a standard, specification, or regulation.

The sponsors do not endorse products or manufacturers. Trademarks or manufacturers' names appear in this report only because they are considered essential to the objective of the document.

Non-discrimination Statement

The University of Iowa does not discriminate on the basis of race, color, age, religion, national origin, sexual orientation, gender identity, sex, marital status, disability, or status as a U.S. Veteran. Inquiries can be directed to the Director of Equal Opportunity and Diversity at the University of Iowa, (319) 335-0705.

Technical Report Documentation Page

1. REPORT NO.	2. GOVERNMENT ACCESSION NO.	3. RECIPIENT'S CATALOG NO.
IGSB Project		

4. TITLE AND SUBTITLE	5. REPORT DATE
A Sediment Composite Fingerprinting Tool: A Field-Based Quantification Method Of The Sediment Origin Within A Water Environment- A Pilot Study	June 2006
	6. PERFORMING ORGANIZATION CODE

7. AUTHOR(S)	8. PERFORMING ORGANIZATION REPORT NO.
A.N. Thanos Papanicolaou, Ozan Abaci, Ranjani Theregowda	

9. PERFORMING ORGANIZATION NAME AND ADDRESS	10. WORK UNIT NO.
IIHR- Hydroscience & Engineering The University of Iowa 300 South Riverside Drive Iowa City, Iowa 52242-1585	11. CONTRACT OR GRANT NO.

12. SPONSORING AGENCY NAME AND ADDRESS			13. TYPE OF REPORT AND PERIOD COVERED
Dr. Mary Skopec Iowa Department of Natural Resources 109 Trowbridge Hall Iowa City, IA 52242-1319 Ames, IA 50010	Iowa Department of Natural Resources 502 E. 9th Street Des Moines, IA 50319		Final Report 14. SPONSORING AGENCY CODE

15. SUPPLEMENTARY NOTES

16. ABSTRACT

The use of WEPP (Water Erosion Prediction Project) in the Upper South Amana catchment in Clear Creek intends to address different fundamental questions regarding the effects of a storm magnitude comparatively to the storm duration as it relates to NPS. This investigation also examines the dependency of the sediment delivery process on landform geometry and cover; the identification of the equilibrium conditions for precipitation, surface runoff; the importance of equilibrium conditions for pollutant transport predictions; and finally how much sediment reaches into the Clear Creek and what are the sediment delivery ratios.

Use of WEPP allows us to indirectly address some other questions: How frequently should we monitor our rivers and lakes in order to establish standards for sediment and nutrients? Is the monthly recording of parameters such as turbidity, TP, an adequate measure for establishing criteria, or more frequent measurements are necessary? Do we need to use NPS predictions obtained under equilibrium conditions to meet different EPA standards?

It was found that the equilibrium WEPP simulations can be used for setting NPS criteria. The strong event simulation can be used to evaluate the efficiency of different BMPs.

Furthermore, the novel capabilities to be sought in the future are applications of WEPP simulations that can dynamically accept responses to online field data and measurements and/or control such measurements. This synergistic and symbiotic feedback control loop between simulation and measurements is a novel technical direction that can open domains in the capabilities of simulations within watersheds and can facilitate the capturing of episodic and catastrophic events. This control loop is not currently available for simulating natural processes.

17. KEY WORDS	18. DISTRIBUTION STATEMENT
Key words: watershed sedimentation, NPS (Non-Point Source) pollution, WEPP (Water Erosion Prediction Project)	No restrictions.

19. SECURITY CLASSIF. (of this report)	20. SECURITY CLASSIF. (of this page)	21. NO. OF PAGES	22. PRICE
None	None		NA

Reproduction of completed page authorized

ACKNOWLEDGEMENTS

This study was funded by the Iowa Department of Natural Resources and Dr. Mary Skopec's research group. Without Mary's help and direct involvement this project will not mature to the point that it has.

The writers are indebted to Dr. Weber, director of IIHR, for contributing matching funds for the installation of equipment/sensors at the IIHR experimental plot located in South Amana, IA. The USDA-Erosion Lab (and Dr. Flanagan) has been of a great assistance to this group. The writers would like to thank Steve Johnston, Ruth Izer, James Martin, Larry Wetjen, Rick Langel, Andy Asell, Casey Khort, Daryl Herzmann and the IIHR Engineering Shop. Dr. Elhakeem has helped in the design of the experimental plot.

The interaction with Mr. Lloyd Trimpe has been very informative and constructive. Without his help this study will not be completed. Additional funding obtained by the USDA –ARS office in Lincoln, NE has helped with the site's instrumentation.

TABLE OF CONTENTS

LIST OF FIGURES

LIST OF TABLES

1. INTRODUCTION

1.1 Problem statement and background

Sediment is currently the leading cause for impairment of streams in the United States, yet a robust methodology to identify and quantify sediment sources in a watershed still has not been developed. To date, we do not have cost-effective ways to monitor all of the Nation's waters and to develop Total Maximum Daily Loads (TMDLs). Sediments are also one of the two major pollutants in the state of Iowa. There is therefore a significant research need for development of an integrated watershed sedimentation framework to improve understanding of sediment transport within a watershed and prediction of sediment fluxes and their nutrient (nitrogen and phosphorus) carrying potential.

This is of critical importance for our state because excessive amounts of nutrients in receiving waters (rivers and lakes) cause the proliferation of algae and aquatic plants, which in turn can restrict the use of water for recreational activities and drinking. High phosphorus loads could also cause the death of fish and other aquatic life. One-third of the 157 waters on Iowa's impaired waters list are impaired by phosphorus.

Various monitoring programs designed and operated to pinpoint troubled areas have been marginally a success because such programs are not appropriately constructed and clearly linked to answer the many questions posed by decision-makers. These programs sample streams on a spatially or temporally limited basis and therefore do not provide enough information to allow decision-makers to identify the most problematic areas of their planning region. In addition, the monitoring results are not effectively utilized for modeling efforts or portrayed in a visual context so that the public and its elected representatives can comprehend the spatial scope and extent of the issues.

Moreover, use of calibrated models can save the state and the agencies a substantial amount of time for identifying the troubled areas and for forecasting the impacts of management practices on water quality. Clearly, new modeling approaches need to be undertaken that facilitate automated measurements at different temporal and spatial scales and able to track non-point sources.

Over the past two decades, different types of models have been developed to address some of the aforementioned issues. Non Point Source (NPS) models describe hydrological and biogeochemical processes such as flow, sediment, nutrients, and chemicals production from hillslopes, and their transport in gullies and rivers. In modeling of such complicated processes, the following aspects of NPS models should be considered: the representation of spatial variability, time scale, and description of hydrologic and environmental processes. NPS models can be classified according to these aspects (see Tables 1a, b, c, d).

Based upon the representation of spatial variability, NPS models can be classified as lumped parameter models and distributed parameter models.

Lumped parameter models (e.g., RUSLE2, CREAMS; EPIC; and GLEAMS) assume that the simulated domain is homogeneous, so that the parameters represent the physical properties for the whole domain. Normally, lumped parameter models are applied to field-sized areas or small homogeneous watersheds. However, in general, a watershed's physical properties such as soils, vegetation, topography, and boundary conditions such as rainfall and other atmospheric inputs, are spatially heterogeneous.

To account for these heterogeneities, spatially distributed models subdivide a watershed into square grids (e.g., ANSWERS; AGNPS; MIKE SHE; and ANSWERS-2000 or topographically derived subareas e.g., SWRRB; KINEROS; HSPF; SWAT; and SWIM). It is assumed that properties within a grid or a subarea are homogeneous. However, different grids or subareas are allowed to be heterogeneous. For this reason, distributed parameter models can represent a watershed more realistically than lumped parameter models.

Depending upon the time scale, NPS models can also be classified as event-based or continuous-time models. Event-based models ANSWERS, AGNPS, and KINEROS are run for a storm event to quantify the short-term impact of management changes. On the other hand, continuous-time models SWRRB, HSPF, SWAT, SWIM, MIKE SHE, ANSWERS-2000, WEPP are run to evaluate the long-term effect of management changes. It is often the case that one seeks the impact of managerial actions over a longer time horizon than a single storm event. For this reason, it is desirable to use continuous-time models that can simulate long term temporal changes that affect runoff and pollutant loss. Please note that some of the continuous models can run in both modes, namely, storm-event and continuous simulations.

Finally, NPS models can be categorized by their description of hydrologic and environmental processes as physically based or conceptual models. Physically based NPS models e.g., WEPP, KINEROS, MIKE SHE, and ANSWERS-2000 describe runoff and the movement of pollutants based on the conservation of mass, momentum, and/or energy equations. Parameters used in these models are related to physical properties, so that they can be estimated from readily available information such as soils, vegetation, topography, geology, and land-use conditions, at public databases. As such, parameters are objectively adjusted in the model according to the variations of physical properties.

On the other hand, conceptual models, such as AGNPS, HSPF, and SWIM, are mostly based upon empirical equations or upon much simplified conservation equations. Hence, their parameters need to be calibrated from historical data, which makes them unsuitable for application to ungauged watersheds.

Based on the critical literature review it is decided that the present research utilizes a physically-based model, WEPP (Water Erosion Prediction Project), to address the NPS issues in a well-monitored site, the south Amana catchment of Clear Creek, IA. WEPP allows the performance of event-based and continuous simulations using the kinematic wave equations for the overland flow component, the Green-Ampt model for wave infiltration and the sediment continuity for surface erosion and deposition. The current work also incorporates other WEPP model capabilities such as the effects of freezing and thawing cycle, the effects of the wind, the presence of a tile drainage network and the ADAPT model equations for modeling phosphorous transport. All these processes occur often in the Midwest and it is considered important to account for their effects via WEPP. A detailed description of WEPP follows after the Objectives section of this report.

The use of WEPP intends to address different fundamental questions regarding the effects of a storm magnitude comparatively to the storm duration as it relates to NPS; regarding the dependency of the delivery process on landform geometry and cover; identification of the equilibrium conditions for precipitation, surface runoff, and sediment delivery; the importance of equilibrium conditions for pollutant transport predictions; how much sediment reaches into the Clear Creek and what are the sediment delivery ratios.

Use of WEPP will also allow us to indirectly address some other questions: How frequently should we monitor our rivers and lakes in order to establish standards for

sediment and nutrients? Is the monthly recording of parameters such as turbidity, TP, an adequate measure for establishing criteria, or more frequent measurements are necessary? Do we need to use NPS predictions obtained under equilibrium conditions to meet different EPA standards?

1.2 Objective and Tasks

To answer these questions, it is our objective to research and develop a methodological framework that encompasses the following areas:

1- Field data collection and data analysis;
2- Development of the phosphorus component;
3- Model set-up and calibration;
4- Performance of continuous simulation to identify the equilibrium condition;
5- Verification of WEPP with field data;
6- Comparison of WEPP with a lumped parameter model RUSLE2;
7- Performance of single storm simulation to evaluate the role of storm magnitude on upland erosion. The event considered here is the highest magnitude event;
8- Comparison of single storm events with continuous simulations.

Table 1a – A summary of existing NPS models

Abbreviation	Full model name	Model developers	Spatial scale	Temporal scale	Structure	Routing
AGNPS	Agriculture Non-Point Source Pollution	USDA-ARS, Young et al. (1987)	Large watershed	Event	Semi-empirical	Yes
AGNPS-UM	Applying the USLE-M within AGNPS	Kinnell (2000)	Large watershed	Event	Semi-empirical	Yes
AnnAGNPS	Annual AGNPS	USDA-ARS (2000)	Large watershed	Continuous	Semi-empirical	Yes
ANSWERS	Areal Nonpoint Source Watershed Environment Response Simulation	USDA-ARS, Beasley et al. (1980)	Large watershed	Event	Physically-based	No
ANSWERS-2000	Areal Nonpoint Source Watershed Environment Response Simulation-2000	USDA-ARS, Bouraoui (1994)	Large watershed	Continuous	Physically-based	Yes
CASC2D-SED	Cascade 2 dimensional sediment model	Colorado State University & USACE (1998)	Large watersheds	Event or continuous	Physically-based	Yes
CREAMS	Chemicals, Runoff and Erosion from Agricultural Management Systems	USDA-ARS and SEA-AR, Foster et al. (1980)	Field/small watershed	Event or continuous	Physically-based	Yes

Table 1b – A summary of existing NPS models

Abbreviation	Full model name	Model developers	Spatial scale	Temporal scale	Structure	Routing
EPIC	Environmental Policy Integrated Climate	USDA-ARS, Williams et al. (1984)	Field	Continuous	Empirical	No
EROSION 3D	Erosion 2D and 3D models	Schmidt et al. (1999)	Small watershed	Event	Physically-based	Yes
EUROSEM	European Soil Erosion Model	European Commission, Morgan et al. (1994)	Small watershed	Event	Physically-based	Yes
GLEAMS	Groundwaters Loading Effects of Agricultural Management Systems	USDA-ARS (1984)	Field/small watershed	Continuous	Physically-based	Yes
HSPF	Hydrological Simulation Program - Fortran	EPA, Johnson et al. (1980)	Basin	Continuous	Semi-empirical	Yes
KINEROS	Kinematic runoff and erosion model	USDA-ARS, Woolhiser et al. (1990)	Small watershed	Event	Physically-based	Yes
LISEM	Limburg Soil Erosion Model	Jetten et al. (1998)	Small watershed	Event	Physically-based	Yes

Table 1c – A summary of existing NPS models

Abbreviation	Full model name	Model developers	Spatial scale	Temporal scale	Structure	Routing
MEDALUS	Mediterranean desertification and land use model	Kirby et al. (1993)	Field/small watersheds	Continuous	Physically-based	Yes
MEDRUSH	Synthesis of MEDALUS catenas	Kirby et al. (1997)	Basin	Continuous	Physically-based	Yes
(R)USLE	(Revised) Universal Soil Loss Equation	USDA-ARS (1978; 1997)	Field	Annual approximations	Empirical	None
RUSLE2	Revised Universal Soil Loss Equation 2	USDA-ARS (2000)	Field	Continuous	Semi-empirical	None
SEMMED	Soil erosion model for Mediterranean regions	de Jong et al. (1991)	Basin	Continuous	Empirical	Yes
SHETHRAN	Sediment transport modeling system	Ewen et al. (2000)	Basin	Continuous	Physically-based	Yes
SWAT	Soil and Water Assessment Tool	USDA-ARS, Arnold et al. (1995)	Basin	Continuous	Empirical	Yes

Table 1d – A summary of existing NPS models

Abbreviation	Full model name	Model developers	Spatial scale	Temporal scale	Structure	Routing
USLE-M	An event version of the USLE	Kinnell and Risse (1998)	Field	Event	Empirical	None
WEPP	Water Erosion Prediction Project	USDA-ARS, Flanagan and Nearing (1995)	Large Watershed	Continuous/Event	Physically-based	Yes

2. THEORETICAL DESCRIPTION OF WEPP

2.1 Watershed Channel Hydrology and Erosion Processes

The WEPP watershed model is a process-based, event or a continuous simulation model developed to predict erosion effects from agricultural management practices and to accommodate spatial and temporal variability in topography, soil properties, and land use conditions within small agricultural watersheds. The model consists of different submodules that are linked to each other, namely, climate, irrigation, hydrology, erosion, soil and plant cropping management. The authors have added the phosphorus component that complements well the sediment component. Figure 1 describes the main submodules of WEPP and also illustrates the data requirements for running WEPP either for continuous or event-based simulations. There are about 7 seven input files that need to constructed. The presence of the WEPP interface makes the data input straightforward. WEPP's built-in defaults allow the user to run the code using input information that match closely the biogeochemical soil properties of the area of interest. Hence, in case of scarce data the user can run the code with the best possible available data obtained directly from the WEPP databases. The WEPP interface is the least comparable to other interfaces (e.g., SWAT, RUSLE) and pretty much self-explanatory. The user manual and the online data information library allow easy access to the on line help.

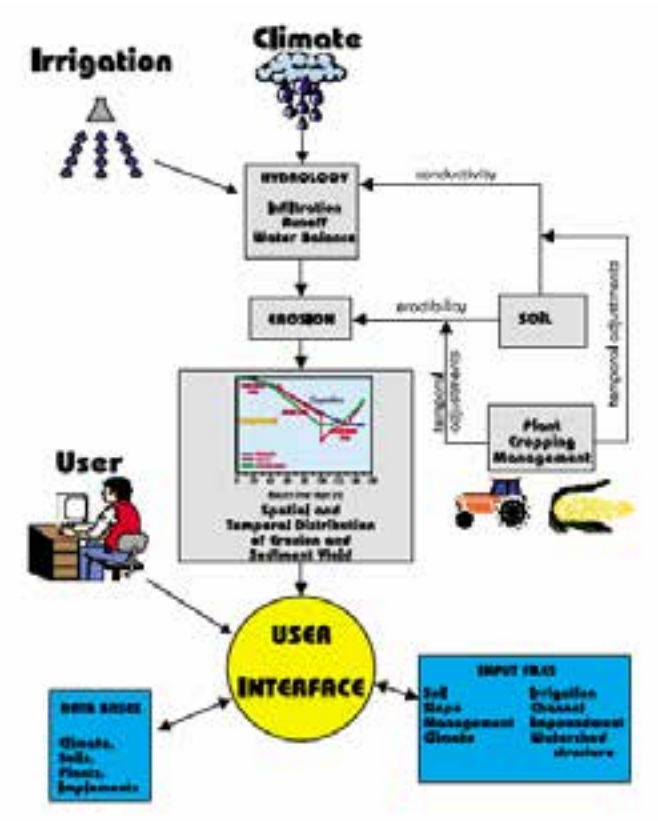

Figure 1 – The main components of WEPP model

WEPP operates per hillslope. In order to employ WEPP in a catchment that consists of several hillslopes the model is run for all the hillslopes and then the results are fed into the channel component of the model. The channel component of the model conveys the NPS outcomes to the catchment outlet. The model then provides the SDR (sediment delivery ratio). Figure 2 depicts the sequence of processes occurring in a hillslope. Interrill flow contributes to the rill by transporting via sheet erosion the material and pollutants into a secondary rill. A secondary rill then, depending on the curvature of the hillslope, either contributes the material directly to the river (convex) or to a primary rill, which in turn it conveys all material into the river (concave).

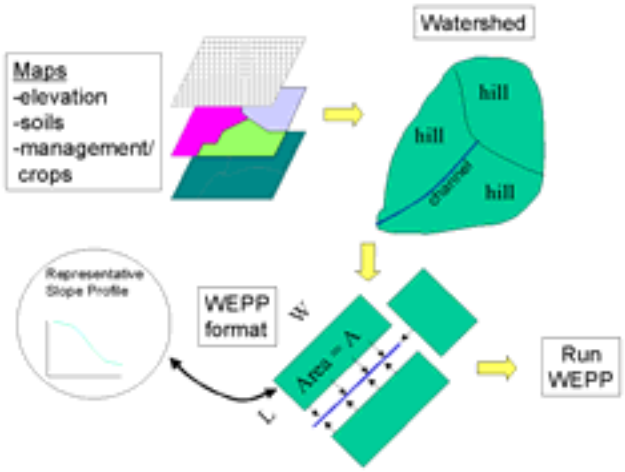

Figure 2 – Depiction of the sequence of processes occurring in a hillslope.

Once the hydrologic and erosion submodules are run for a hillslope, the hillslope hydrologic and erosion outputs (e.g., runoff volume, peak runoff rate, and sediment concentration) is stored in a hillslope-watershed pass file and then read in and used by the channel component. WEPP model is capable of: 1) identifying zones of sediment deposition and detachment within constructed channels (e.g., grassed waterways or terraces) or concentrated flow (ephemeral) gullies; 2) accounting for the effects of backwater on sediment detachment, transport, and deposition within channels; and 3) representing spatial and temporal variability in erosion and deposition processes as a result of agricultural management practices. It is intended for use on small agricultural watersheds (up to 260 ha) in which the sediment yield at the outlet is significantly influenced by hillslope and channel processes.

The channel component is divided into the hydrology and erosion components wherein channel hydrology component computes infiltration, evapotranspiration, soil water percolation, canopy rainfall interception, and surface depressional storage in the same manner as the hillslope hydrology component. Rainfall excess is calculated using a Green-Ampt Mein-Larson (GAML) infiltration equation. Two methods are provided for calculating the peak runoff rate at the channel (subwatershed) or watershed outlet. Channel water balance calculations are performed after the channel runoff volume has been computed. The channel water balance and percolation routines are identical to those used in the hillslope component. Input from the climate, infiltration, and crop growth routines are used to estimate soil water content in the root zone, soil evaporation, plant transpiration, interception, and percolation loss below the root zone.

The watershed model erosion component assumes that watershed sediment yield is a result of detachment, transport, and deposition of sediment on overland (rill and interrill) flow areas and channel flow areas, that is, erosion from both hill slope areas and concentrated flow channels must be simulated by the watershed version. Flow depth and hydraulic shear stress along the channel are computed by regression equations based on a numerical solution of the steady-state spatially-varied flow equation. Outlet conditions for the channel are assumed to be controlled by a downstream uniform flow, critical depth, or a structure having a known rating curve (e.g., an experimental flume). Subcritical flow is assumed unless the user specifies that slope of the energy gradeline (friction slope) equals the channel (bed) slope. Channel computations are made assuming triangular or naturally eroding channel sections.

Detachment, transport, and deposition are calculated by a steady-state solution to the sediment continuity equation. The flow detachment rate is proportional to the difference between: 1) the flow shear stress exerted on the bed material and the critical shear stress; and 2) the transport capacity of the flow and the sediment load. Net detachment occurs when flow shear stress exceeds the critical shear stress of the soil or channel bed material and when sediment load is less than transport capacity. Net deposition occurs when sediment load is greater than transport capacity. A nonerodible boundary is assumed to exist at some depth below the bottom of the channel. When a channel erodes to the nonerodible boundary, the channel widens and erosion rate decreases with time until the flow is too shallow to cause detachment. In the subsequent sections the most prominent components of WEPP are discussed.

2.2 Peak Discharge

WEPP uses two methods of computing the peak discharge; a semi-analytical solution of the kinematic wave model (Stone et al., 1992) and an approximation of the kinematic wave model. The first method is used when WEPP is run in a single event mode while the second is used when WEPP is run in a continuous simulation mode.

2.3 Kinematic wave model

The kinematic equations for flow on a plane are the continuity equation

$$\frac{\partial h}{\partial t} + \frac{\partial q}{\partial x} = v$$

and a depth-discharge relationship

$$q = \alpha h^m$$

where, h = depth of flow (m),

q = discharge per unit width of the plane ($m^3.m^{-1}.s^{-1}$),

α = depth-discharge coefficient,

m = depth-discharge exponent, and x = distance from top of plane (m).

The Chezy relationship is used for overland flow routing in WEPP so,

$$\alpha = CS_o^{0.5}$$

where, C = Chezy coefficient ($m^{0.5}.s^{-1}$) and m =1.5.

The initial and boundary conditions are

$$h(x,0) = h(0,t) = 0$$

The above equations are solved using the method of characteristics. The method involves rewriting continuity and depth-discharge relationship as simple ordinary differential equations on characteristic curves in the t-x plane. The equations for depth and distance along a characteristic c (t,x) at a given time are

$$\frac{dh}{dt} = v(t)$$

$$\frac{dx}{dt} = \alpha m h(t)^{m-1}$$

The characteristic, defines a locus of points in the time-space plane on which the flow depth is computed by equations for depth and distance characteristic. This equation is integrated w.r.t. x (x_1= distance (m) on a characteristic at time t_i, h_1 = depth (m) on a characteristic at time t_1), and t (t_1 and t_2 = limits of integration (s)).

2.4 Approximate method of calculating peak flow

The surface hydrology component supplies the erosion component with the volume and peak rate of runoff and the duration of rainfall excess. An approximation was developed on the basis of the relationship among the time to kinematic equilibrium, the duration of rainfall excess, D_v (s), the peak rainfall excess rate, v_p ($m.s^{-1}$), and the average rainfall excess rate, v_a ($m.s^{-1}$).

2.5 Constant rainfall excess

For constant rainfall excess, v_a ($m.s^{-1}$), the flow depth and discharge rate increases during the period $t < t_e$ and is constant for $t \geq t_e$. If the duration of the rainfall excess is less than t_e, then the maximum flow depth, h_p (m), is

$$h_p = v_c D_v$$

Substituting maximum flow depth in depth-discharge relationship, using the definition of t_e, and simplifying, the peak discharge, q_p ($m.s^{-1}$), is

$$q_p = v_c \left[\frac{D_v}{t_e} \right]^m \text{ for } D_v < t_e$$

When the duration of rainfall excess is greater than the time to kinematic equilibrium (i.e. equilibrium), then the peak flow rate is simply

$$q_p = v_c \text{ for } Dv > t_e$$

The above discharge equations can be generalized by defining the following dimensionless quantities as

$$q_* = \frac{q_p}{v_c}$$

$$t_* = \frac{t_e}{D_v}$$

The peak flow rate becomes,

$$q_* = t_*^{-m} \qquad \text{for } t_* \geq 1$$

$$q_* = 1 \qquad \text{for } t_* < 1$$

2.6 Variable rainfall excess

Using the generalized peak discharge equations we define average rainfall rate as

$$v_a = \frac{V_t}{D_v}$$

where, V_t = total rainfall excess depth (m)

Using the average rainfall rate

$$t_a = \left[\frac{L}{\alpha v_a^{m-1}} \right]^{1/m}$$

Redefining the dimensionless quantities in generalized peak discharge as

$$q_* = \frac{q_p}{v_a}$$

$$t_* = \frac{t_a}{D_v}$$

and defining a dimensionless rainfall excess rate

$$v_* = \frac{v_a}{v_p}$$

The WEPP model was run using the kinematic routing procedure to produce values of q_*, t_*, and v_* for a range of rainfall characteristics, soil types, initial conditions, and depth-discharge coefficients. Plotting if simulations suggest the following relatively simple equations which could be used to approximate the peak discharge

$$q_* = t_*^{-m} \text{ for } t_* \geq 1$$

$$q_* = \frac{1}{t_*} \text{ for } 1 > t_* \geq t_{**}$$

$$q_* = \frac{1}{v_*} - 0.6\frac{1 - v_*}{v_*} t_* \text{ for } t_{**} > t_* \geq 0$$

Combining the last two equations, substituting t_{**} for t_* and solving for using the quadratic formula as

$$t_{**} = \frac{1 - \sqrt{1 - 2.4(v_* - v_*^2)}}{1.2(1 - v_*)}$$

slope term (0.6) changes if Manning's relationship is used to compute α

2.7 Recession infiltration

To account for the infiltration during the recession of the hydrograph, WEPP uses a relationship among the final infiltration rate, average rainfall excess rate, and total rainfall excess volume. By defining the following dimensionless quantities

$$Q_* = \frac{Q_v}{V_{t*}}$$

$$f_* = \frac{f_f}{v_a}$$

where, Q_v= adjusted runoff depth (m) and f_f = final infiltration rate ($m.s^{-1}$) at the last time of non-zero rainfall excess rate.

The reduction in runoff volume is computed as

$$Q_* = \frac{1}{m+1}\frac{f_*+1}{f_*}t_*^{-m} \text{ for } t_* \geq \left[\frac{f_*+1}{f_*}\right]^{1/m}$$

$$Q_* = 1 - \frac{m}{m+1}\left[\frac{f}{f_*+1_*}\right]^{1/m} t_* \text{ for } t_* < \left[\frac{f_*+1}{f_*}\right]^{1/m}$$

2.8 Runoff duration

The WEPP Model uses the steady-state sediment continuity equation as a basis for erosion computations. As a result, the steady-state runoff discharge rate is assumed to be the peak discharge rate computed by the kinematic routing procedure or the approximate method described above. Under this assumption, the computed runoff duration would not maintain continuity between the peak discharge rate and the runoff volume. In order to maintain continuity, an effective duration, D_e (s), is computed in the WEPP surface hydrology component and is used in the rill erosion computations:

$$D_e = \frac{Q_v}{q_p}$$

2.9 Subsurface Lateral Flow

In WEPP, we assume that the soil layer with water content in excess of field capacity, θ_{FC} (water held at 33KPa tension for most soils), is subjected to percolation to a lower layer and to lateral flow. Such a soil layer is referred to as a drainable layer hereafter. The mass continuity equation in finite difference form for a given hillslope can be written as:

$$\frac{S_2 - S_1}{d_2 - d_1} = P_e - (D + ET)L - \frac{q_1 + q_2}{2}$$

Where, S = drainable depth of water (m),

d = day of simulation,

P_e= percolated water to the drainable layer ($m.d^{-1}$),

D = seepage out of the drainable layer ($m.d^{-1}$),

ET= actual evapotranspiration from drainable layer ($m.d^{-1}$),

L = length (m) and

q = discharge from the hillslope per unit width (m)

Since the WEPP water balance simulates daily P_e, D and ET, calculation of subsurface lateral flow is done on a daily basis (see Chapter 5 for more detail). The drainable volume of water is calculated by

$$S = H_o \theta_o \, L/2$$

where, Ho is the thickness of drainable layer normal to slope (m), and

θ_o is drainable water and is calculated as

$$\theta_d = \theta - (\theta_{FC} - \theta_a)$$

where θ = total soil moisture ($m^3.m^{-3}$),

θ_{FC}= soil water content at field capacity ($m^3.m^{-3}$), and

θa= entrapped air ($m^3.m^{-3}$).

Subsurface lateral flow from a hillslope of 1 meter width is calculated using the equation

$$q = 86400\, H_o K_{o(\theta)} \sin(\alpha)$$

where, q = subsurface lateral flow ($m.d^{-1}$),

K_e = horizontal hydraulic conductivity ($m.s^{-1}$) at moisture content θ and

α= average slope angle

2.10 Surface Drainage

In the WEPP model, surface drainage is characterized by the depressional storage. Depressional storage is directly related to soil surface micro-relief features and generally enhanced by various soil mechanical practices, such as tillage. Maximum depth of depressional storage (*cm*) is calculated using the following equation:

$$DS = 0.112\, R_r + 0.031 R_r^{\,2} - 0.012\, R_r S_p$$

where, R_r = random roughness (*cm*), and

S_p= average slope steepness (%).

The amount of runoff leaving the hillslope, while depressional storage is filling, is determined using the equation:

$$Q_i = \frac{DS}{PR} V_i \qquad FL < DS$$

$$Q_i = V_i \qquad FL \geq DS$$

where Q = runoff rate leaving the profile ($cm.h^{-1}$),

V = excess rainfall rate ($cm.h^{-1}$),

i = interval of rainfall intensity distribution, and

FL= accumulated amount of excess rainfall filling the depressional storage (*cm*).

The volume of water (V_{wat}) filling the depression storage for each rainfall event can be obtained by subtracting Q from V.

$$FL = \sum_{i=1}^{n} (Qi - Vi) \qquad FL < DS$$

2.11 Subsurface Drainage

The algorithm for simulation of subsurface flow to artificial drain tubes or ditches in WEPP draws heavily from DRAINMOD. The subsurface flux into drain tubes or ditches depends on the soil hydraulic conductivity, drain spacing and depth, soil depth and water table elevation. Assuming flow in the saturated zone only, drainage flux in any simulation day is calculated using the equation:

$$Q_i add = \frac{8K_{zy}h_e M_d + 4K_{zy}M_d^2}{L^2{}_p}{}_i$$

where Q_{dd}= drainage flux per unit width ($cm.d^{-1}$),

K_{zy}= effective hydraulic conductivity for subsurface drainage ($cm.d^{-1}$),

M_d = midpoint water table height (cm),

L_d= distance between drains (cm), d is the day of simulation, and

h_e = equivalent depth (cm), calculated with the Moody equations

For uniform flow conditions, the Darcy-Weisbach friction coefficient, f, is given as

$$f = \frac{8gRS}{V^2}$$

where, g = acceleration due to gravity ($m.s^{-2}$),

R = hydraulic radius (m),

S = average slope, and

V = is flow velocity ($m.s^{-1}$)

Separate estimates of Darcy-Weisbach friction coefficients are made for rill and interrill areas.

A total equivalent friction coefficient for cropland, f_e, is then computed as an area weighted average of the rill and interrill areas using the relationship

$$f_e = f_r A_r + f_i (1 - A_r)$$

where, f_r = total friction coefficient in the rill,

f_i = total friction coefficient for the interrill region, and

A_r = fraction of the total area in rills.

2.12 Roughness Coefficients for Cropland Rills

Shear stress in rills is divided into two parts; one that acts on the soil to cause detachment and the other that acts on exposed residue or other surface cover and thus, not active in terms of soil detachment. The portion of the shear stress which acts on the soil and causes erosion is proportional to the ratio of the friction coefficient for the soil to the total friction coefficient (soil plus cover). If cover exists in the rill, the portion of total shear acting on the soil will only be a fraction of the total shear stress in the rill. The total friction coefficient for rill areas, f_r is given as

$$f_r = f_{sr} + f_{cr} + f_{live}$$

where, f_{sr} = friction coefficient for rill surface roughness=1.11,

f_{cr} = friction coefficient for rill surface residue, and

f_{live} = friction coefficient for living plants which act to slow runoff.

The following equation for predicting f_{cr} was developed from the laboratory data,

$$f_{cr} = 4.5 r_c^{1.55}$$

where, r_c = fraction of the rill covered by residue material.

A linear function was assigned based upon the canopy height of the plant, *canhgt*, compared to its maximum height, h_{max}:

$$f_{live} = canhgt / h\max) f_{livmx}$$

The maximum value of f_{live} (f_{livmx}) assumed for alfalfa and grasses were 12.

2.13 Roughness Coefficients for Cropland Interrill Areas

Interrill surface roughness, surface residue cover, standing plant material, and gravel and cobble material may all influence the total friction coefficient for the interrill area, *fi* , since

$$f_i = f_{si} + f_{ci} + f_{bi} + f_{live}$$

Where, f_{si}= friction coefficient for interrill surface roughness,

f_{ci} = friction coefficient for interrill surface cover,

f_{bi} = friction coefficient for a smooth bare soil, and

f_{live}= friction coefficient for living plants as defined earlier.

Form roughness elements may be quite large compared to flow depth on interrill areas. Finkner (1988) related form roughness elements to friction coefficients using the relationships

$$f_{s\,i} = 0.5\, f_o^{\,1.13} \exp^{-3.09(1.0-r_i)-f_{bi}}$$

where,

$$f_o = \exp^{3.0-5.04\exp(_i-161r_o)}$$

and r_o = initial random roughness of a freshly tilled soil (*m*),

r_i = ratio of random roughness at some later time to r_o, and

f_o = friction factor for a freshly tilled surface in the absence of cover.

The friction coefficient for interrill surface cover, f_{ci} , is given by

$$f_{ci} = 14.5 i_c^{1.55}$$

where, i_c is the fraction of the interrill area covered by nonmoveable residue.

The friction coefficient for a smooth bare soil on an interrill area, f_{bi} , is represented as

$$f_{bi} = 4.07$$

2.14 Flow Shear Stress

Shear stress of rill flow is computed at the end of an average uniform profile length by assuming rectangular rill geometry. The uniform profile is defined as a profile of constant or uniform gradient, $\overline{S}$, that passes through the endpoints of the profile. Rill width, *w* (*m*), may either be input by the user or may be calculated using,

$$w = 1.13 Q_e^{0.303}$$

where, Q_e = rill flow rate

Depth of flow in the rill is computed with an iterative technique using the Darcy-Weisbach friction factor of the rill, the rill width, and the average slope gradient. Hydraulic radius, *R* (*m*), is then computed from the flow width and depth of the rectangular rill. Shear stress acting on the soil at the end of the uniform slope, τ_{fe} (*Pa*), is calculated using the equation

$$\tau_{fe} = \gamma R \sin(\alpha)\left(\frac{f_s}{f_t}\right)$$

where, γ = specific weight of water ($kg.m^{-2}.s^{-2}$),

α = average slope angle of the uniform slope,

f_s = friction factor for the soil, and *ft* is total rill friction factor.

The ratio of f_s / f_t represents the partitioning of the shear stress between that acting on the soil and the total hydraulic shear stress, which includes the shear stress acting on surface cover.

2.15 Sediment component

WEPP solves the sediment continuity equation for rill erosion and provides results of rill width and depth within a hillslope profile. A comprehensive review of the model formulation is available in Foster et al. (1995). The driving sediment transport equation for rill erosion in the model includes the steady-state sediment continuity equation for a hillslope given as:

$$\frac{dG}{dx} = D_f,$$

where G is sediment load (kg/s/m) and D_f is rill erosion rate (kg/s/m^2). D_f is either detachment in rills when the applied hydraulic shear stress exceeds the critical shear stress of the soil and when the sediment load is less than the sediment carrying capacity. Rill detachment is:

$$D_f = K_r(\tau_f - \tau_c)\left(1 - \frac{G}{T_c}\right),$$

where K_r is a rill erodibility parameter (s/m), τ_f is bed shear stress exerted by the fluid (Pa), τ_c is the critical shear stress (Pa), and T_c is sediment transport capacity (Kg/s/m). Net deposition in the rill is computed when sediment load, G, is greater than sediment transport capacity, T_c. The equation for deposition follows:

$$D_f = \frac{\beta V_f}{q}(T_c - G),$$

where V_f is the effective fall velocity for the sediment (m/s), q is unit discharge in the rills (m^2/s), and β is a raindrop-induced turbulent coefficient. WEPP allows for specification of climate, agriculture management, and soil parameters that correspond to the conditions of the Upper Palouse. From the WEPP analysis, the maximum depth of rill erosion, D_{mf}, may be calculated after budgeting deposition and detachment as well as the sediment yield, S_y, from the rills.

2.16 Phosphorus component

The sediment transport calculations are complemented with estimations of phosphorus. The load of phosphorus is decomposed and calculated here as the summation of the dissolved phosphorus and the undissolved phase. The concentration of phosphorus in the surface layer of soil available for runoff and percolation in µg/g is calculated as follows:

$$C = CPLAB \times \exp\left(\frac{-(F - ABST)}{CPKD\left(\frac{1 - POR}{2.65}\right) + POR} \right)$$

where CPLAB is the concentration of labile phosphorus in µg/g, based upon the dry weight of the soil, CPKD is the partitioning coefficient, F is total storm infiltration or rainfall minus runoff in cm, POR is the porosity of the surface soil layer, and ABST is the initial abstraction from rainfall in cm.

$$ABST = 0.2(SAT - SW)$$

where SAT is volumetric water content at saturation in cm/cm and SW is volumetric water content in cm/cm. The total storm infiltration is calculated as follows:

$$F = P - Q$$

where P is the precipitation depth in cm. The initial abstraction from rainfall, ABST, is obtained by use of the below relation

$$Q = \frac{(P - ABST)^2}{(P - ABST) + (SAT - SW)} = \frac{(P - 0.2 \times (SAT - SW))^2}{(P - 0.2 \times (SAT - SW)) + (SAT - SW)}$$

$$Q = \frac{(P - 0.2 \times (SAT - SW))^2}{(P + 0.8 \times (SAT - SW))}$$

An average Bray P is obtained from Klatt et al. (2003) as 35 μg/g for a very similar agricultural catchment in northern Iowa. Sharpley et al. (1984) related CPLAB in μg/g to Bray P in case of highly weathered soils as follows:

$$CPLAB = 0.14 \times BP + 4.2$$

CPKD is related to the percent clay in soil as

$$CPKD = 1 + 2.5 \times Clay\%$$

The concentration of phosphorus in water is calculated as follows:

$$CPLABW = \frac{C \times \beta}{1 + CPKD \times \beta}$$

where β is the extraction coefficient for phosphorus. By using the Leonard et al. (1987) relations of β to CPKD

β = 0.5	for $CPKD \le 1.0$
β = 0.5 98×exp (-0.179CPKD)	for $1.0 \le CPKD \le 10.0$
β = 0.1	for $CPKD \ge 10.0$

The labile phosphorus in runoff in kg/ha, is

$$ROLP = 0.1 \times CPLABW \times Q$$

where Q is the surface runoff depth in cm.
Sediment associated labile phosphorus in kg/ha is calculated as

$$SEDLP = 0.1 \times ER \times SY \times CPKD \times CPLABW$$

where ER is the enrichment ratio of sediment and SY is the sediment yield in kg/ha.

3. METHODOLOGY

In order to evaluate the importance of a particular event or a sequence of events on non-point source pollution estimates, two main different scenaria were considered, viz., 1) continuous simulations and 2) single storm events.

Overall eleven continuous simulations were performed for a period of 2 - 200 years in order to identify the periods that soil transport and phosphorous fate reach equilibrium. These extensive runs are also valuable for examining the sensitivity of WEPP and for verifying the predictive ability of the model compared to historic data and the RUSLE2 predictions.

On the other hand, the single storm simulation was performed for the strongest magnitude event for the years of 2004 and 2005. The hypothesis behind the latter run is that high magnitude events matter the most to the transport and fate of phosphorous. Two specific events were investigated in a great detail. The first simulation focused on model calibration and verification. The second simulation focused on the strongest event during the year 2004-2005 in order to provide direct comparisons of WEPP and phosphorous predictions with the IOWATER phosphorus field measurements.

Because one of the intentions of this study is to develop a blueprint methodology useful for future studies, a detailed description of the methodological steps considered here with respect to model initial set-up, calibration and verification is provided. As WEPP incorporates several layers of modulus for land use and management, application of fertilizers and pesticides, Digital Elevation Models (DEM), climatic conditions and biogeochemical properties of soils, the data required for all these modulus are described in a detail below.

3.1 Land uses and management data

Figure 3 provides a plan view of the land use managements in the Upper South Amana catchment during seasons 2004 and 2005. The maps were obtained by the NRCS office in Williamsburg, IA. The most common land use is corn-soybean rotation i.e., 85% of the land use. Other land uses are CRP, hay and pasture. Table 2 summarizes the timeline of operations during the 2 year rotation period (2004-2005).

Table 2 – Upper South Amana catchment corn-soybean rotation timeline

Date	Operation
01-May-04	Plant soybean (high fertilization level)
25-May-04	Herbicide application
25-Jun-04	Kill perennial
25-Sep-04	Harvest soybean (high fertilization level)
01-Nov-04	Tillage - Anhydrous application
01-Apr-05	Tillage (Field cultivator, sweeps 12"-20")
15-Apr-05	Herbicide application
15-Apr-05	Tillage (Field cultivator, sweeps 12"-20")
01-May-05	Plant corn (high fertilization level)
01-Oct-05	Harvest corn (high fertilization level)

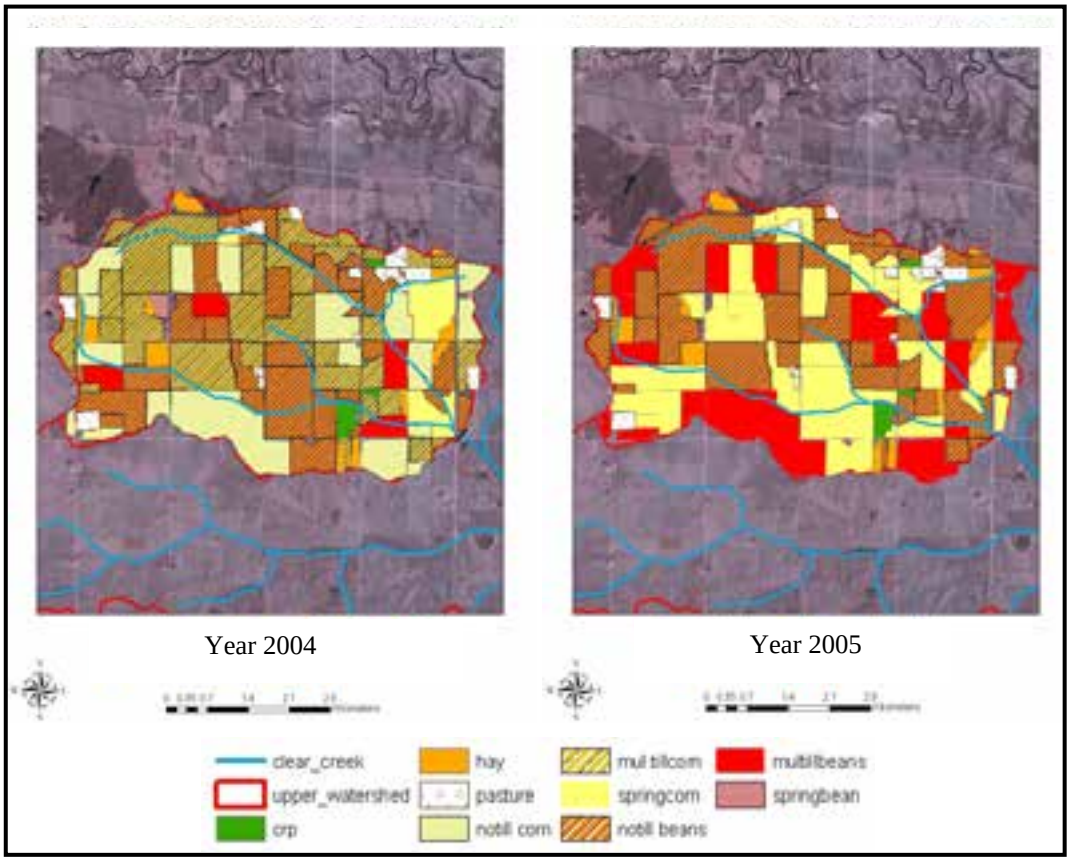

Figure 3 – Upper South Amana catchment land use maps for 2004 and 2005

Tables 3 and 4 summarize the tillage information during the rotation period. Specifically, Table 3 refers to the anhydrous application with closing disks and Table 4 refers to the field cultivator application where 12″ - 20″ sweeps are typically applied.

Table 3 – Tillage anhydrous application with closing disks

Parameter	Value
Percent residue buried on interrill areas for fragile crops (0-100%)	30
Percent residue buried on interrill areas for non-fragile crops (0-100%)	30
Number of rows of tillage implement	8
Ridge height value after tillage (inches)	3
Ridge interval (inches)	20
Percent residue buried on rill areas for fragile crops (0-100%)	30
Percent residue buried on rill areas for non-fragile crops (0-100%)	30
Random roughness value after tillage (inches)	2
Surface area disturbed (0-100%)	50
Mean tillage depth (inches)	3

Table 4 – Tillage field cultivator application with 12″ - 20″ sweeps

Parameter	Value
Percent residue buried on interrill areas for fragile crops (0-100%)	20
Percent residue buried on interrill areas for non-fragile crops (0-100%)	20
Number of rows of tillage implement	20
Ridge height value after tillage (inches)	2
Ridge interval (inches)	20
Percent residue buried on rill areas for fragile crops (0-100%)	20
Percent residue buried on rill areas for non-fragile crops (0-100%)	20
Random roughness value after tillage (inches)	2
Surface area disturbed (0-100%)	50
Mean tillage depth (inches)	2

Table 5 provides the initial conditions considered for the eleven continuous simulations. All simulations start on January 1st 2004 and have the same initial conditions regarding the land use and management, application of fertilizers and pesticides, Digital Elevation Models (DEM), climatic conditions and biogeochemical properties of soils. This table also includes information about canopy cover, tillage residue, landform characteristics such as ridge height and roughness, rill geometry, dead root mass and submerged residue mass, snow depth and depth of frost and thaw.

Table 5 – Initial conditions on January 1st, 2004

Parameter	Value
Initial Plant	Corn
Bulk density after last tillage (g/cub. cm)	1.1
Initial canopy cover (0-100%)	60
Days since last tillage (days)	255
Days since last harvest (days)	90
Initial frost depth (inches)	2
Initial interrill cover (0-100%)	60
Initial residue cropping system	Annual
Cumulative rainfall since last tillage (inches)	30
Initial ridge height after last tillage (inches)	0.5
Initial rill cover (0-100%)	60
Initial roughness after last tillage (inches)	2
Rill spacing (inches)	20
Rill width type	Temporary
Initial snow depth (inches)	0
Initial depth of thaw (inches)	2
Depth of secondary tillage layer (inches)	0
Depth of primary tillage layer (inches)	0
Initial rill width (inches)	1
Initial total dead root mass (lbs/acre)	3569
Initial total submerged residue mass (lbs/acre)	892.1

Table 6 summarizes the initial conditions considered during the most intense single storm event in 2004 and 2005. These conditions were also considered for the phosphorus calculations.

Table 6 – Initial conditions for the strongest storm of 2004-2005 (06/25/05 storm)

Parameter	Value
Initial Plant	Corn
Bulk density after last tillage (g/cub. cm)	1.1
Initial canopy cover (0-100%)	30
Days since last tillage (days)	70
Days since last harvest (days)	265
Initial frost depth (inches)	0
Initial interrill cover (0-100%)	30
Initial residue cropping system	Annual
Cumulative rainfall since last tillage (inches)	2
Initial ridge height after last tillage (inches)	2
Initial rill cover (0-100%)	30
Initial roughness after last tillage (inches)	2
Rill spacing (inches)	20
Rill width type	Temporary
Initial snow depth (inches)	0
Initial depth of thaw (inches)	0
Depth of secondary tillage layer (inches)	2
Depth of primary tillage layer (inches)	0
Initial rill width (inches)	1
Initial total dead root mass (lbs/acre)	2000
Initial total submerged residue mass (lbs/acre)	800

Table 7 shows the initial condition parameters for the September, 2005 storm simulations on the calibration plot shown in Figure 4. During the period of simulation the plot, found in the Upper South Amana, maintained bare soil conditions.

Figure 4 – Experimental Station at South Amana, IA

Table 7 – Initial conditions for the calibration simulation (September 2005)

Parameter	Value
Initial Plant	N/A
Bulk density after last tillage (g/cub. cm)	1.1
Initial canopy cover (0-100%)	0
Days since last tillage (days)	N/A
Days since last harvest (days)	N/A
Initial frost depth (inches)	0
Initial interrill cover (0-100%)	0
Initial residue cropping system	N/A
Cumulative rainfall since last tillage (inches)	20
Initial ridge height after last tillage (inches)	0
Initial rill cover (0-100%)	0
Initial roughness after last tillage (inches)	0
Rill spacing (inches)	0
Rill width type	Temporary
Initial snow depth (inches)	0
Initial depth of thaw (inches)	0
Depth of secondary tillage layer (inches)	0
Depth of primary tillage layer (inches)	0
Initial rill width (inches)	0
Initial total dead root mass (lbs/acre)	N/A
Initial total submerged residue mass (lbs/acre)	0

3.2 Pesticides and fertilizers data:

3.2.1 Pesticides:

The two main combinations of pesticide applied to corn within the Upper South Amana catchment are the following: (i) Cinch ATZ *and* Harness-extra and (ii) Gaurdsman Max *and* Distinct. Cinch ATZ and Harness-extra is the primary combination used in the catchment and it is applied in 2/3rd of the total number of available corn fields. Cinch ATZ is applied at the rate of 2 pint/acre during April; and Harness-extra is applied at the rate of 4.6 pint/acre in June. The remaining 1/3rd of the corn fields are treated with Gaurdsman Max and Distinct combination. Gaurdsman Max is applied at the rate of 4.6 pint/acre in April and then Distinct is applied at the rate of 0.25 pint/acre in June. The "surface application" method is adopted to disperse these pesticides to the crops, thus retention time of these pesticides on the ground is one to two months i.e., no herbicide residue is left on the soil surface for the subsequent year.

A single combination is used for the soybeans within the catchment. Either Pursuit is applied at the rate of 2.5 pint/acre or Prowl at 3.0 pint/acre during late-April. Later, pesticide Roundup is applied twice at a rate of 1.375 pint/acre, once in May and then in June. These pesticides are also surface applied, with a retention time on the surface soil being a month, therefore, no remnants exists on the top surface after a month of their application.

In case of CRP and Pasture, 2 4-D Amine or Tartan 22K is applied at a rate of 1.5 pint/acre or 0.5 pint/acre respectively, sometime between April and July. No herbicide application is done for hay.

Insecticide application is mainly dependent on insect population. In case of corn, Aztec – 10.92 pint/acre or Force 3G – 6.77 pint/acre is used by 1/3rd of the farming population, between April and July. The remaining 2/3rd farmers do not apply insecticides. Insecticides are mixed with corn seeds and applied via planters (30″ rows).

In case of hay, either Pounce – 0.25 pint/acre or Baythroid – 0.125 pint/acre is applied in mid-June. The insecticide is sprayed on the plant. In case of soybeans, CRP and pasture there is no insecticide application.

3.2.2 Fertilizers:

Five percent (5%) or lesser of the farming population uses manure and the remaining uses commercial fertilizers in the Upper South Amana area. As manure provides Nitrogen (N), Phosphorus (P) and Potassium (K), farmers who apply manure prefer lower application rates than those described below. N is applied only to corn each year, while P and K are applied once in two years to the corn-soybean rotation. N and P-K mixture are not applied simultaneously.

In case of corn, anhydrous ammonia is injected at the rate of 150 lb/acre by the 3/4th of farmers. Approximately 2/3rd of them apply it in November and the remaining 1/3rd prefer to apply it in April. Depth of incorporation during injection is 6″. The remaining 1/4th apply 150 lb/acre on the surface in April. N applied to corn each year lasts till the subsequent year. Since soybean produces N internally no external application is required.

Ninety percent (90%) of the farmers apply P-K mixture via surface application either in November or April. The remaining 10% is injected it into the soil (depth of incorporation = 3″) during April. Application rate in both the cases is 100 lb/acre. P-K mixture lasts approximately for 2 years.

3.3 Digital Elevation Models:

Digital Elevation Models were constructed from elevation data obtained in 1999 from the Iowa Geological Surveying Bureau. The resolution of the data is 30 m. Figure 5 provides the topographical information obtained via the USGS National Elevation Dataset (NED). This figure illustrates the watershed structure, the hillslope gradients and the channel gradients.

There are two divisions in the catchment; they are the North and South Divisions. Northern division has overall steeper rills, channels and hillslopes. The average hillslope gradient is 4.3% and average rill slope is the 2.4% in Upper South Amana, whereas the creek slope is 0.7%.

Understanding the topography of the Upper South Amana catchment is of vital importance in constructing WEPP model to correctly represent the pathways of flow and sediment in Upper South Amana. Typically, flow and sediment pathways are determined by the gradient of hillslope and the curvature shape. Convex shaped hillslopes tend to direct the flow towards the center of the hillslope, where flow becomes concentrated and leads to the formation of a primary rill defined in WEPP as a channel. In a nutshell, for convex hillslopes, secondary rills collect the flow from the interill areas and transport it to the channel. The channel then carries the flow and sediment into the creek.

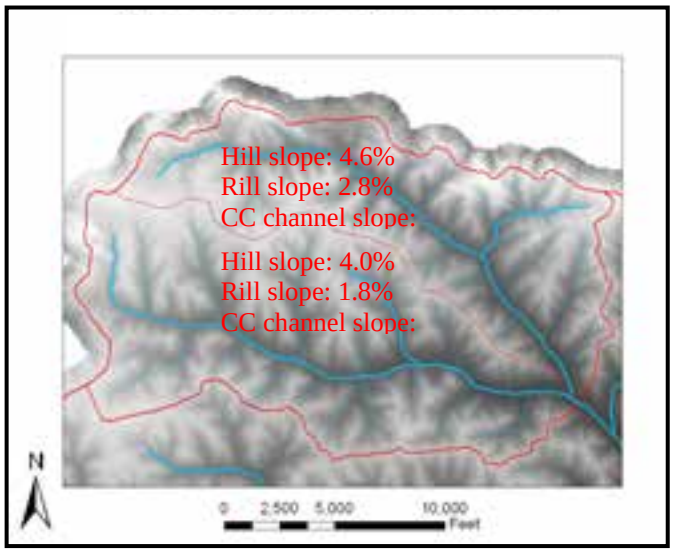

Figure 5 – Upper South Amana catchment Digital Elevation Model

In the case of concave shaped hillslopes, flow does not follow the same pathways as described in convex shaped hillslopes. In concave hillslopes, flow is directed to the creek via rills that are almost parallel to each other due to flow gravitational affects. Therefore,

identification of convex and concave hillslopes is of paramount importance in setting the WEPP model correctly. A misrepresentation of the natural flow pathways may lead to an error that in most cases is greater than 80%. To avoid the pitfall, a GIS tool was utilized to map the flow directions within the Upper Watershed Amana catchment. Figure 6a illustrates the utility of this tool in South Amana and Figure 6b demonstrates the flow distribution for a convex hillslope 80% of the hillslopes in Clear Creek are of convex shape. Hence, primary and secondary rills are considered during the catchment scale simulations.

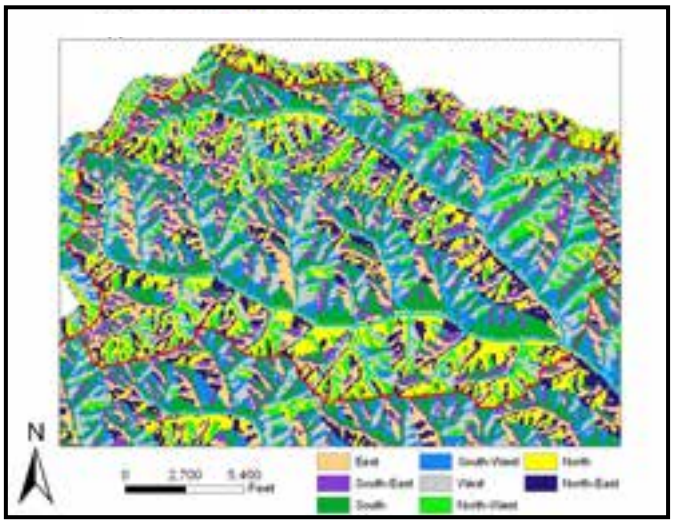

Figure 6a – Flow directions within the catchment

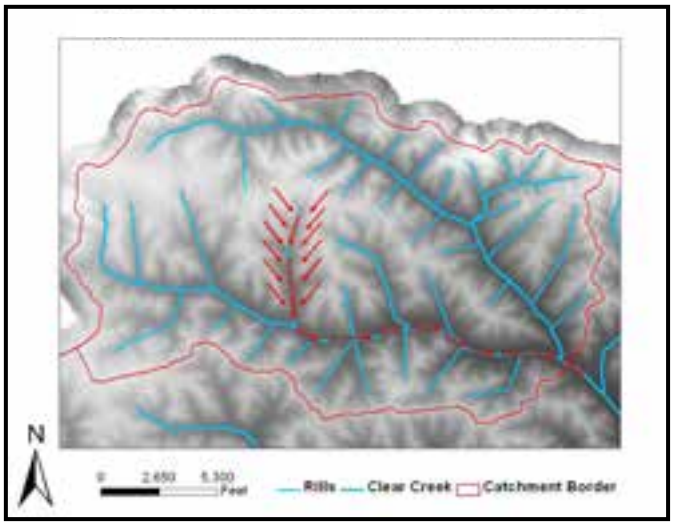

Figure 6b – Erosion pathway within the catchment

Based on the above discussion, 113 hillslopes were considered. For the simulation, it was ensured that the size of each hillslope did not exceed 250 ha. This threshold value was recommended by the WEPP developers. The reason behind this recommendation is that

WEPP cannot adequately simulate flow roughness and sediment transport occurring in primary and secondary rills and channels that are greater than 2 ft wide (i.e., first order channels). Figure 7 illustrates the 113 hillslopes, the main rills and the creek. The outlet of the catchment is located at the downstream confluence of the North and South fork of Clear Creek.

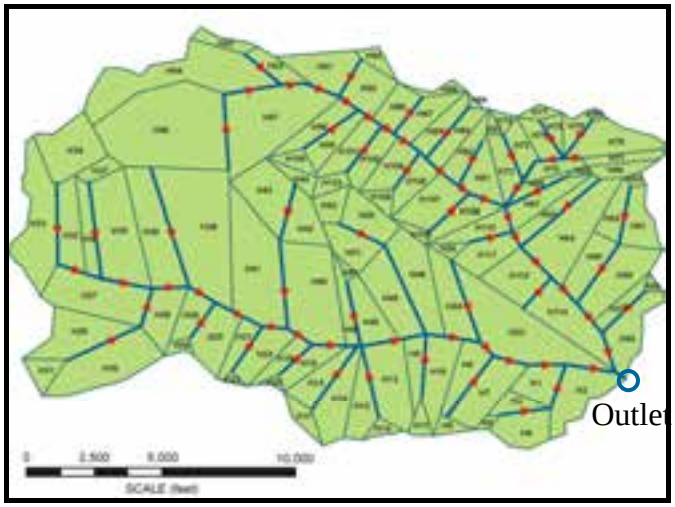

Figure 7 – WEPP watershed model structure

The results for the continuous simulations or the single storm simulations will be obtained by running WEPP for each of the 113 hillslopes. The same applies for the single storm simulation.

3.4 Climatic Conditions:

Climatic data are very important for WEPP, because they provide information about precipitation, solar radiation, temperature, storm duration, maximum intensity. Storm amount and storm duration are important for determining surface runoff and subsequently sediment erosion and transport of the pollutants attached to sediments. The climatic data were compiled using the probabilistic weather software CLIGEN, a stochastic weather data generator. Table 8 provides the average, minimum, maximum temperature for each month, the solar radiation per month and the average precipitation per month based on continuous simulations extended over a period of 45 years.

Table 8 – Monthly average climate statistics for Williamsburg, IA

Variable / Month	Jan	Feb	Mar	April	May	June	July	Aug	Sept	Oct	Nov	Dec
T_{max} (^oC)	-1.4	1.6	8.1	16.8	23	27.8	29.8	28.7	24.6	18.5	9	1.3
T_{min} (^oC)	-9.7	-8	-3.1	3.5	9.8	15.1	17.5	16	11.3	5	-1.8	-7.5
Solar Rad (langleys)	175	253	329	410	490	548	503	472	384	284	195	147
Precip. (mm)	25.5	22.1	52.5	82.5	103.6	119.1	116.3	103.2	94.7	62.2	61	33.9

These monthly averaged data are utilized as input values to CLIGEN in order to generate daily precipitation, temperature and solar radiation data for the closest weather station to the site located in Williamsburg, IA. Due to the large volume of information the daily precipitation and solar radiation data generated by CLIGEN and used in the continuous simulations are not included here in. Characteristics of the strongest storms during 2004-2005 are provided in Table 9.

Table 9 – Characteristics of the strongest storms during 2004-2005

Date	Storm Amount	Strom Duration	Maximum Intensity	% Duration to peak intensity
---	[mm]	[hr]	[mm/hr]	---
09/14/04	62.3	5	40.4	35
07/02/04	27.8	2	35.2	10
09/13/04	36.3	4	33.5	50
09/05/04	10.4	1	31.5	50
09/15/04	23.0	2	27.8	80
06/20/05	40.5	2	74.1	88
06/25/05	**70.5**	**3**	**57.9**	**25**
06/08/05	41.2	1	50.8	25
06/04/05	50.5	2	50.7	75
09/24/05	30.3	3	49.3	8

Those data were obtained from the Iowa Environmental MESONET, at Iowa State University in Ames, IA. Table 10 summarizes selected storm events obtained during September of 2005. These storm events are used for model calibration purposes.

The calibration precipitation data are obtained via a tipping bucket device which provides automatic records of precipitation that are transferable through wireless technology. The precipitation data are obtained exactly at the same location where the plot

is found. It is anticipated that future calibrations of WEPP over the experimental plot (base soil) will be based on the precipitation records obtained via the tipping bucket.

Table 10 – Characteristics of the storms during September of 2005

Date	Storm Amount	Strom Duration	Maximum Intensity	% Duration to peak intensity
---	[mm]	[hr]	[mm/hr]	---
09/05/05	0.5	1	0.5	50
09/06/05	19.1	1	45.4	50
09/12/05	3.2	3	3.3	25
09/17/05	12.4	6	5.4	25
09/18/05	14.7	1	31.4	25

3.5 Biogeochemical Properties of Soil:

Detailed biogeochemical information was obtained from historic data collected by USGS back in 1967 and from current survey of the Upper South Amana during the project duration. Specifically, GIS layers for soil mineralogy, permeability, organic matter, pH and Cation Exchange Capacity (CEC) were provided. Although these data are historic and therefore of unknown resolution they provide strong background information about the biogeochemical conditions in the whole Clear Creek watershed including Upper South Amana Catchment. The soil map layer (Figure 8a) shows silty clay loam as the dominant soil texture in Upper South Amana, with fine sandy loam patches along the Upper Northern border neighbouring to the Iowa River Basin.

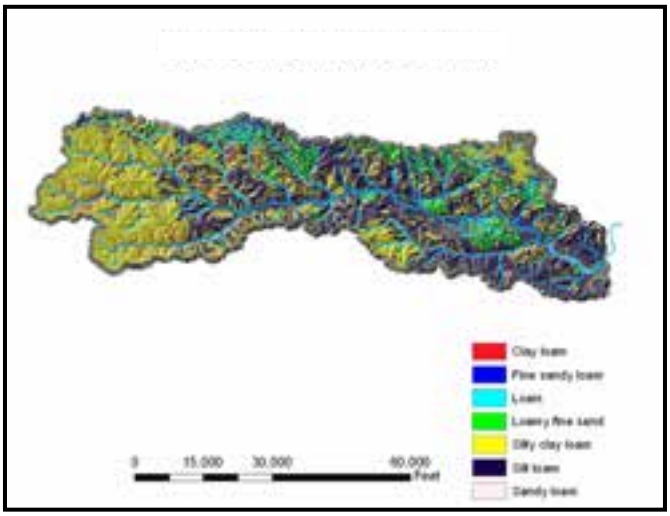

Figure 8a – Soil texture map of Clear Creek watershed

In addition a detailed analysis of the soil composition at selected sampling locations found in Upper South Amana via sieve and hydrometer analysis confirm the information shown in Figure 8a. Atterberg's limits (plasticity limit and liquid limit) show the existence of about 13% clay in the Upper soil horizon. Further analysis using the X-ray (XRD – X-ray diffraction) technique shows that there is a mixed layer of clay minerals. These are smectite, vermiculite, kaolinite and illite. All of these minerals are found to be abundant, but smectite was determined to be dominant mineral. This implies that soils in the South Amana area are sensitive to soil moisture conditions. Specifically, when water percolates through the ground, the smectite mineral tends to expand. Figure 8b demonstrates the average permeability measured in inches per hour in the catchment and the whole Clear Creek watershed.

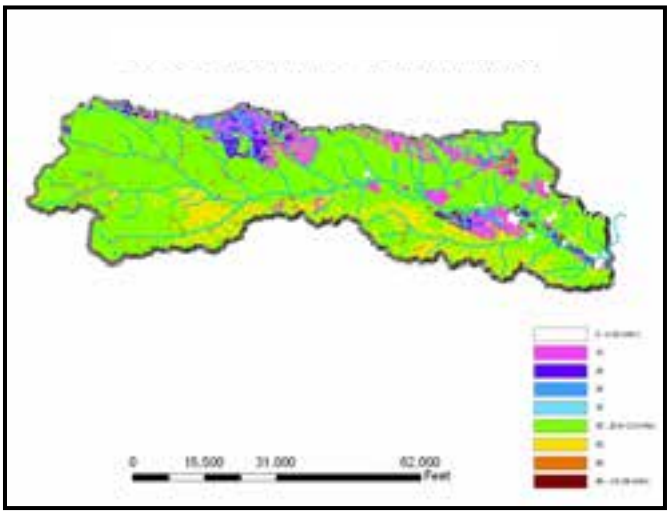

Figure 8b – Permeability map of Clear Creek watershed

The permeability layer reveals that infiltration through the ground is overall occurring in a homogeneous manner. Rainfall infiltrometer measurements performed in the South Amana area provide similar values for the permeability. Figure 8c demonstrates that the organic matter in South Amana is within 3-4%. Figure 8d & 8e provide the average values for the pH of soils and CEC (Cation Exchange Capacity).

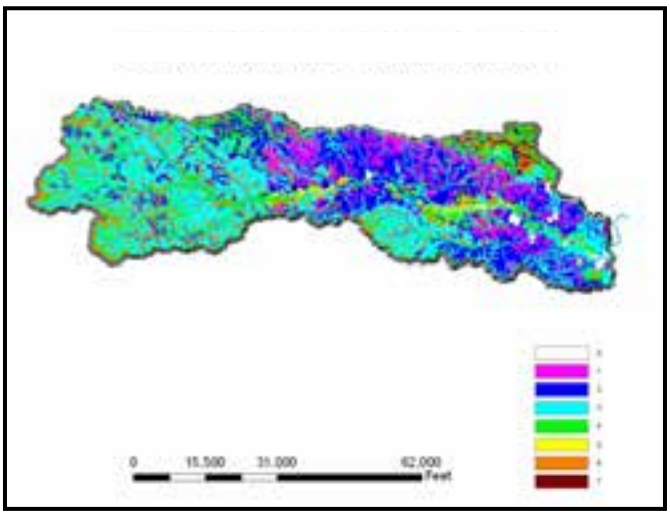

Figure 8c – Organic Matter (%) map of Clear Creek watershed

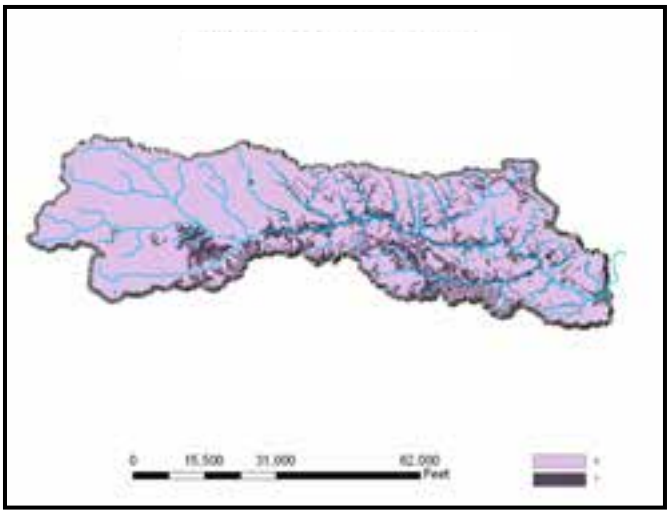

Figure 8d– Soil pH map of Clear Creek watershed

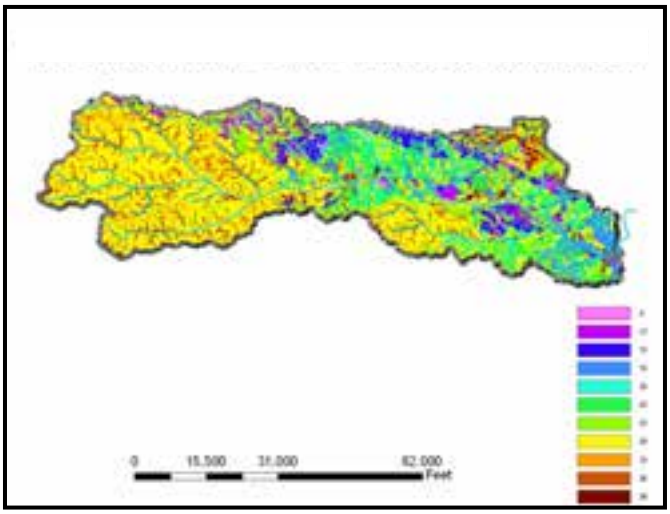

Figure 8e – CEC (meq/100g) map of Clear Creek watershed

The average pH value is about 6, suggesting that point contact exists between adjacent particles, makes the connection between the clay particles susceptible to rainfall impact or fluid action. CEC values demonstrate a soil that is active in exchange with potassium, calcium, magnesium elements. Detailed biogeochemical properties of the catchment soil are summarized in Table 11.

Table 11 – Biogeochemical properties of the catchment soil

Property	**Units**	**Corn**	**Soybean**	**CRP**	**Floodplain**	**Bank**
Geological						
Silt	%	65.4	59.2	63.3	70.0	66.4
Clay	%	29.5	34.7	30.3	26.4	26.7
Sand	%	5.10	6.10	6.40	3.60	6.90
Water Content	%	21.5	20.0	25.36	16.1	18.35
Specific Gravity	---	2.56	2.73	2.46	2.54	2.50
Plastic Limit	%	26.70	27.00	24.20	32.35	24.36
Liquid Limit	%	36.34	38.07	38.59	47.00	37.68
Chemical						
pH	---	7.70	7.75	6.05	6.45	6.95
Buffer pH	---	7.30	7.35	6.70	7.00	7.13
Exch. K	cmol/kg	0.749	0.639	0.431	1.154	0.248
Exch. Ca	cmol/kg	21.21	31.13	10.82	12.52	12.00
Exch. Mg	cmol/kg	3.63	3.26	2.18	3.36	2.98
Exch. Na	cmol/kg	0.07	0.10	0.05	0.03	0.04
Zn	g/kg	0.0021	0.004	0.0011	0.0052	0.0016
Fe	g/kg	0.070	0.098	0.116	0.140	0.088
Mn	g/kg	0.013	0.010	0.018	0.021	0.017
Organic Matter	g/kg	43.55	54.85	53.85	74.70	30.52
Total C	g/kg	23.85	30.05	29.59	40.96	16.71
Total N	g/kg	2.061	1.964	2.672	3.496	1.638
NO_3-N	g/kg	0.0036	0.0022	0.0026	0.0027	0.0038
NH_4-N	g/kg	0.0013	0.0140	0.0040	0.0050	0.0080
CEC	cmol/kg	25.660	35.120	17.089	17.069	15.266
SAR	√(cmol/kg)	0.0191	0.0236	0.0205	0.0123	0.0135
Biological						
Photo Pathway	---	C4	C3	C3	---	---

It can be seen that the corn site soil, though similar to soybean site soil has characteristic values slightly higher among the cultivated soils, but floodplain soil (uncultivated) has highest characteristic values compared to all types of soils. Higher water content among the samples is seen for CRP - 25.4% & corn soil - 21.5%. This can be explained by the vegetation cover, which retains infiltration i.e., root spread of grasses in the topsoil compared to corn. In another way we can also say the evapotranspiration process is low in smaller plants (grasses) thus preventing water loss due to canopy height. Row crops such as corn, soybeans and potatoes offer relatively little cover during the early growth

stages and thereby encourage erosion. Atterberg's values accord with the concept that water is more apt to flow out of wet soil than from one low in moisture. This relates erosion to strength of soil particle bonding and weakening of this bond due to water particles. More water it can withhold, denser the soil tends to be and thus, lower shear required for soil erosion. Cation exchange for the corn and soybean soils were among the highest (25.7 and 35.1 cmol/kg), indicating liming to sustain neutral pH fertilizer application, making these soils more stratified with clay, whereas the uncultivated soils have lower CEC values (15.3 – 17.1 cmol/kg). Increasing CEC has an effect on the erodibility factor, but as CEC increases above 10 cmol/kg, it has negligible effect on the erodibility factor. Also, critical stress has been found to increase with CEC up to a point and then stay constant. Sodium adsorption ratio (SAR) is low for all soils which produce interparticle attraction explaining flocculation, which makes it easier for the particle to be eroded unless the bonding between them is strong. Diethylene Triamine PentaAcetate (DTPA) micronutrients (Zn, Fe, and Mn) in the floodplain are high, due to deposition of eroded particles from upland. Organic matter estimated from the total C varied between ~3% for bank soil to ~7% for floodplain soil. Even 1-3% of organic matter can reduce erosion up to 20-33%. But, in the study area organic matter is depreciating in the tilled soil, indicating a probability of decreasing below 3% due to intensive agricultural practices in future. Organic carbon in corn varies as its photosynthetic pathway (metabolism), which is C_4. Corn soil and bank soil due to lower organic content are apparently less stable as SOM is the major binding agent observed. Similarly, for soybean NO_3-N is lower, as nitrates are converted by legumes at a faster rate. CRP being Brome grass belongs to the C_3 pathway which is seen in the results of organic matter/total C and NO_3-N, where both soils have closer values.

Table 12 provides the properties of the soil used in the WEPP model for simulating hillslope erosion for continuous and single storm events.

Table 12 – WEPP model soil characteristics

Sand	Clay	Silt	Organic	CEC	Rock	Albedo
(%)	(%)	(%)	(%)	(meq/100g)	(%)	---
3.0	30.0	64.5	3.0	28.0	2.5	0.23

Table 13 provides information about the initial saturation level, the interrill and rill erodibility factors , critical fluvial erosion strength and conductivity.

Table 13 – WEPP model soil erodibility characteristics and saturation level

Init. Sat. Level	K_i	K_r	τ_c	K
(%)	($kg.s/m^4$)	(s/m)	(Pa)	(mm/hr)
75	6037461	0.007	3.5	0.74

The interrill and rill erodibility factors K_i, K_r respectively are reflective of the soil strength and initial saturation level (soil water content). Both erodibility and initial saturation level are related to the fluvial erosional strength, which is defined as the strength at which incipient motion condition occurs. The fluvial erosional strength is the summation of the electromagnetic Coulomb forces and of the biological factors. Bacteria and plant roots tend to increase the value of fluvial erosional strength, while the freezing-thawing cycle has the opposite effect. For the simulation performed here, the critical erosional strength value is considered to be 3.5 Pa. This value agrees with values reported in the literature and is applicable to primary and secondary rills. These values are not the same for the sediment found in the Clear Creek.

Table 14 provides an estimate of the Manning's Roughness Coefficient and of the critical shear stress (or equivalently the critical erosional strength) for the sediment found in Clear Creek. The value of the critical erosional strength of the sediment bed in Clear Creek is considered to be 5 Pa.

Table 14 – WEPP model channel erodibility characteristics

Parameter	Value
Manning roughness coefficient for bare soil in channel	0.025
Total Manning roughness coefficient allowing for vegetation	0.040
Channel erodibility factor (s/m)	0.000125
Channel critical shear stress (Pa)	5.0
Depth to non-erodible layer in mid-channel (m)	0.5
Depth to non-erodible layer on sides (m)	5.0

3.6 Calibration methodology:

An important component of this research is the calibration of WEPP. The calibration process typically occurs in a well controlled environment. In the present study an experimental plot that is 36ft long and 40ft wide was considered within the South Amana area. The plot was located in the floodplain of the Clear Creek and was designed by PI

Papanicolaou and his team as a continuous precipitation, runoff, sediment, water quality monitoring station. Figures 9a and 9b illustrate the site.

Figures 9a, 9b – Erosion pins placed within the experimental station

Fence posts were used to define the boundaries of the plot and the downstream end of the experimental plot was designed to be a V-shaped. Plexiglass walls formed the walls of the V-shape to direct the surface runoff to the exit of the plot where a Parshall flume is located. Figure 9c demonstrates the experimental station, the contour lines of the plot and the contour lines of the farm road separating the experimental plot from the corresponding hillslope.

Fence posts and the erosion pins were placed with well structured arrangement at a distance of 4ft apart from the neighbouring pins and the outlet of the experimental plot, where the Parshall flume is located.

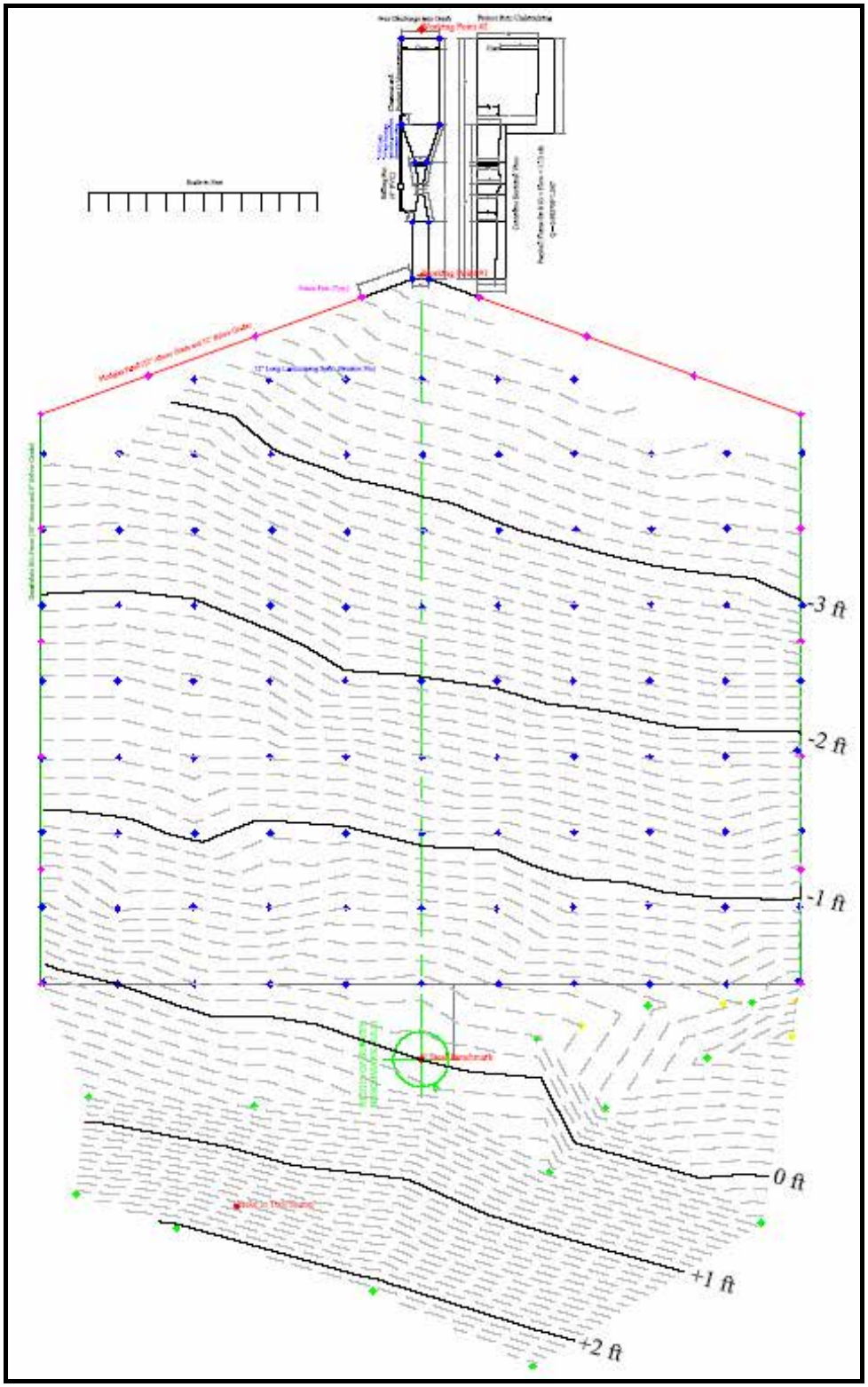

Figure 9c – Plan view of experimental station

The Parshall flume shown in Figure 9d allowed the collection of sediment via a sediment trough. The sediment trough captured bedload. A SIGMA portable water sampler, shown in Figure 9e, was used to capture the suspended load. The Parshall flume was of

known dimensions, thus providing surface runoff estimations without performing any form of calibration.

Figure 9d – Parshall flume

Figure 9e – SIGMA portable water sampler

Figures 9f and 9g provide a view of the tipping bucket device that is wireless and transfers automatically data to IIHR's website.

Figures 9f, 9g – Tipping bucket

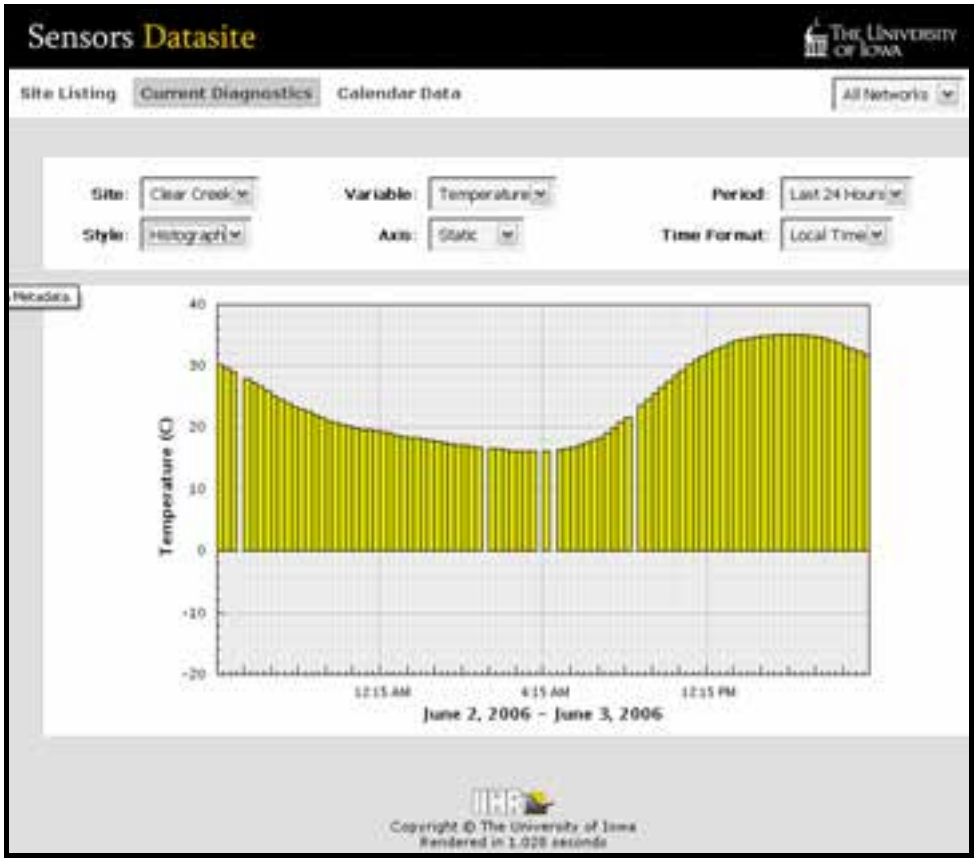

Figures 9h – IIHR Sensors datasite

Figure 9h is an example of the IIHR website and shows the temperature variation. Figures 9a and 9b illustrate that the soil at the site is bare and fallow. This was considered important for calibrating the model because no sediment lag is present at this plot. The plot surface soil has a minimal roughness. The erosion pins were submerged to the ground in September 2005 by causing minimal disturbance. Erosion measurements were collected at

September 20th of 2005, right after the occurrence of 5 sequential storms with initial storm date being September 5th and final storm date was September 18th (Table 10). Erosion was quantified by measuring the exposure of the erosion pins. SDR was determined by the SIGMA device and the Parshall flume. Table 7 summarizes the land use parameters used for the model calibration. These parameters accurately reflect the initial conditions at the site.

Figure 9i illustrates a side view of the experimental plot as it is simulated in WEPP. The hillslope consists of 3 parts: the CRP land, a road and the experimental plot at the downstream end of the hill. The input parameters used in WEPP have been described in Section 3.5. During calibration we tested the input values for erosional strength, erodibility and conductivity. The simulation from WEPP produced a net sediment erosion that is equivalent to 0.75 inches in depth. This compares favourably to the 1 inch depth net erosion that was measured on September 2005.

Specifically, WEPP predicted a 50 kg/m^2 net soil loss. Converting the soil loss to units of depth, this gives a 0.75 inches net erosion depth.

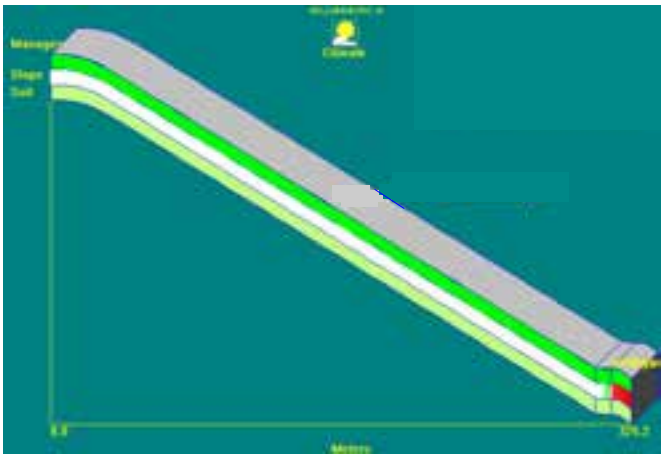

Figure 9i – WEPP simulation of experimental plot

4. RESULTS

The results section is organized as follows: First, the continuous simulations are presented. The continuous simulations were performed to identify the equilibrium conditions and the yearly averaged sediment erosion and sediment yield for the South Amana area. Figure 7 illustrates the 113 hillslopes that were considered in the continuous simulation. Comparisons between simulation results and field measurements are provided for the continuous simulations. These comparisons are complemented with additional

comparisons between WEPP, a physically based model, and RUSLE2, a lumped parameter model.

Second, following the continuous simulations, phosphorus simulations were performed for the most intense storm recorded on June 25th 2005. A comparison between the single storm and the IOWATER sampling program is provided.

4.1 Continuous Simulation:

Table 15 provides the water and sediment discharges at the outlet of the South Amana area for a period of 2 – 200 years. These extensive simulations are necessary in order to identify the conditions that flow and sediment equilibrium occurs. Table 15 indicates that equilibrium conditions occur for the flow component at about 50 years and for the sediment at about 100 years.

Table 15 – Continuous simulations results

Period	Precipitation volume in contributing area	Water Discharge	Sed. Discharge
(yrs)	(m^3/yr)	(m^3/yr)	(t/yr)
2	16674642	3095818	8533.1
5	16773949	4144822	8324.0
10	18496094	5368892	22972.0
15	18287984	5323152	19392.6
17	18239658	5378618	21050.9
20	18873940	5636397	26536.9
25	18877145	5775717	26334.9

Table 15 – Continuous simulations results (continued)

Period	Precipitation volume in contributing area	Water Discharge	Sed. Discharge
(yrs)	(m^3/yr)	(m^3/yr)	(t/yr)
50	18962205	5963838	32340.6
100	18953447	6044190	25376.3
150	18826416	6008677	23002.3
200	18725598	5954759	24601.4

Figures 10a, 10b and 10c provide the variation of the precipitation volume, water discharge and sediment discharge respectively. Figures 10a and 10b illustrates that there is strong correspondence between precipitation volume and surface water discharge.

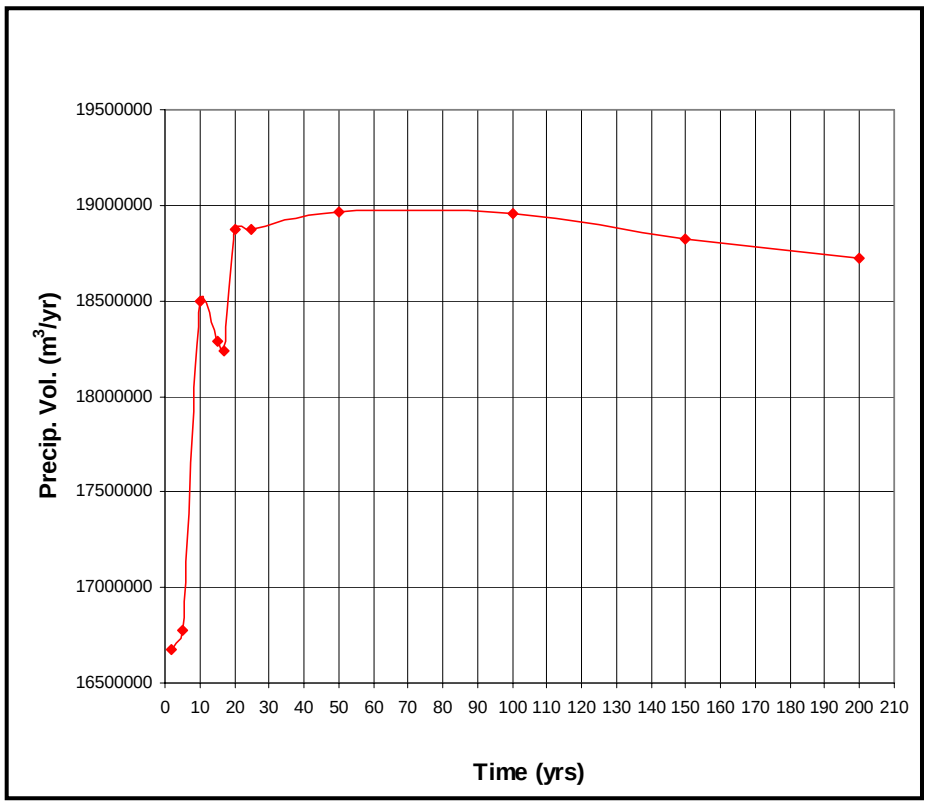

Figure 10a – Precipitation volume variation in contributing area

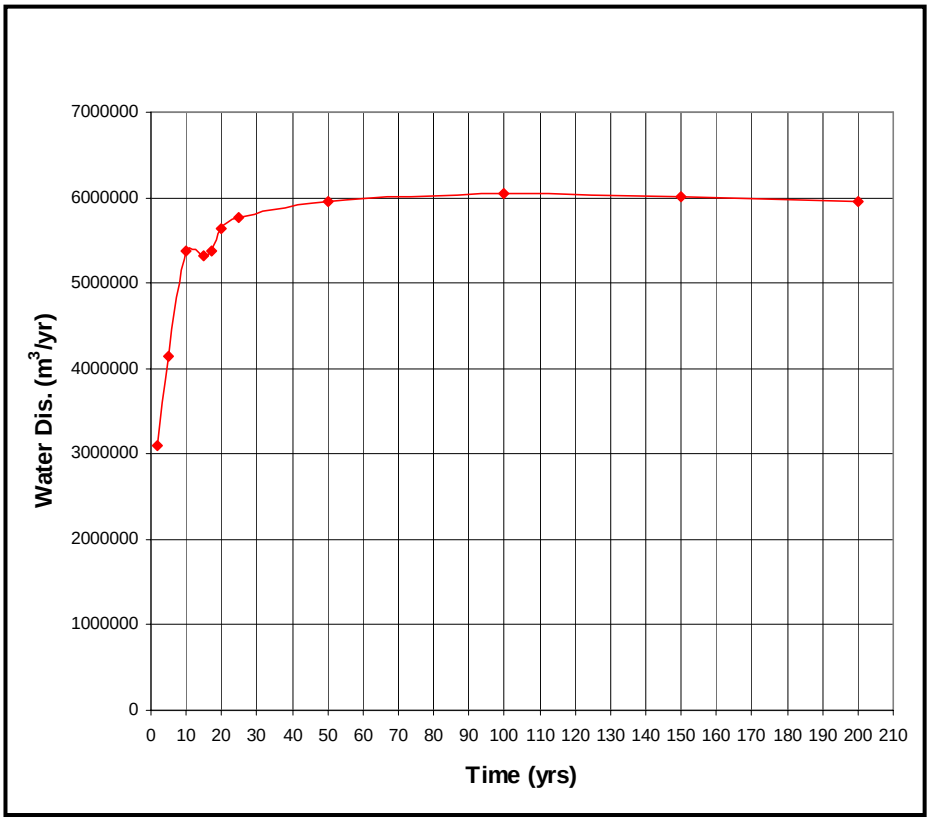

Figure 10b – Average annual water discharge from outlet

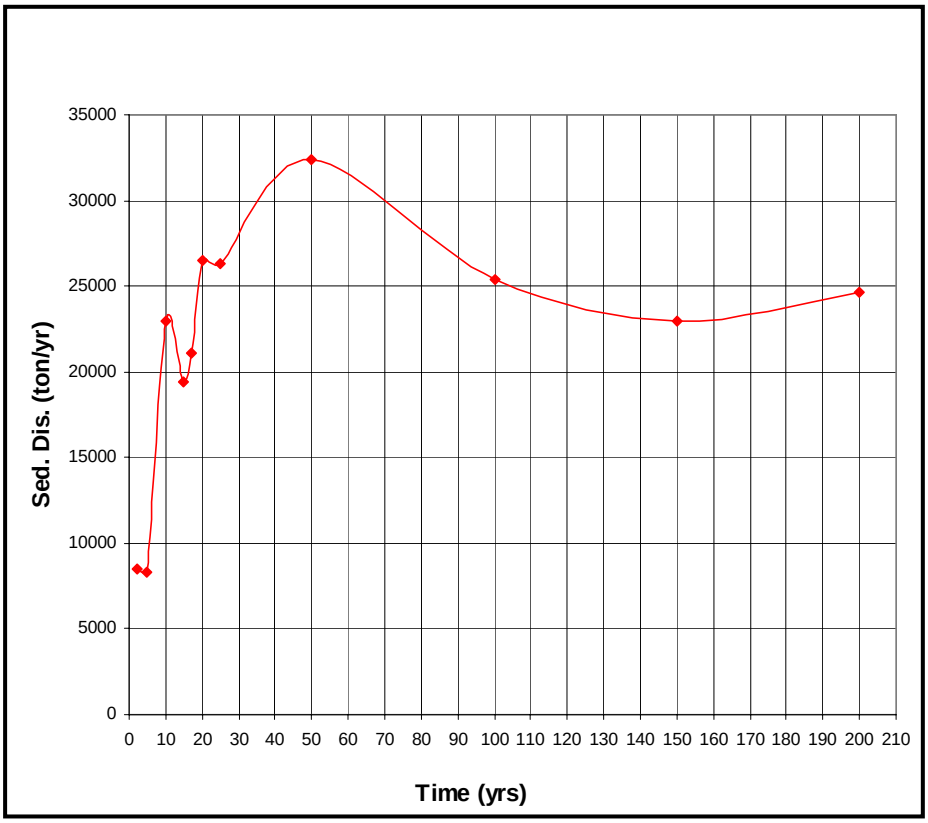

Figure 10c – Average annual sediment discharge from outlet

These figures show that after the 50th year, equilibrium conditions start to prevail with respect to surface water discharge. Figure 10c illustrates a similar pattern but it shows that there is a gap of 50 years in order for the sediment to reach equilibrium condition. This is attributed to the fact that the relation between sediment discharge and flow is highly nonlinear. Physically, this nonlinearity is attributed to the presence of vegetation, roughness, land form irregularities, shape of the hillslope and the randomness in precipitation and moisture conditions. All of these parameters affect the delivery time of sediment and in some cases introduce a lag time between flow and sediment. Figures 11a, 11b, 11c and 11d provide the time series of interrill erodibility factor, rill erodibility factor, fluvial erosional strength and effective hydraulic conductivity. It is shown that after the first 2 years of simulations the input values for these properties remain constant, which suggests that the initial input variables set into the model based upon the calibration process are accurate.

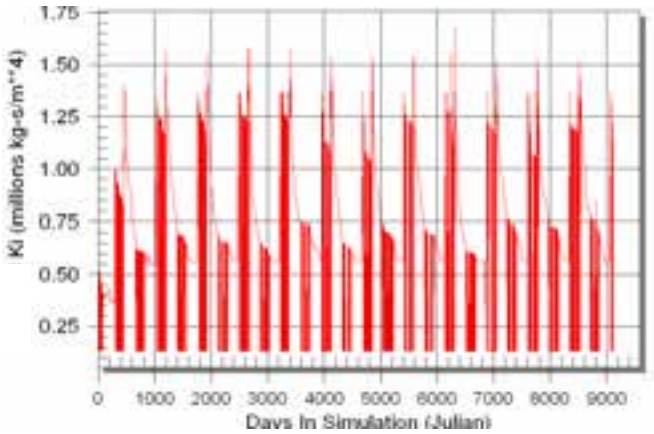

Figure 11a – Interrill erodibility

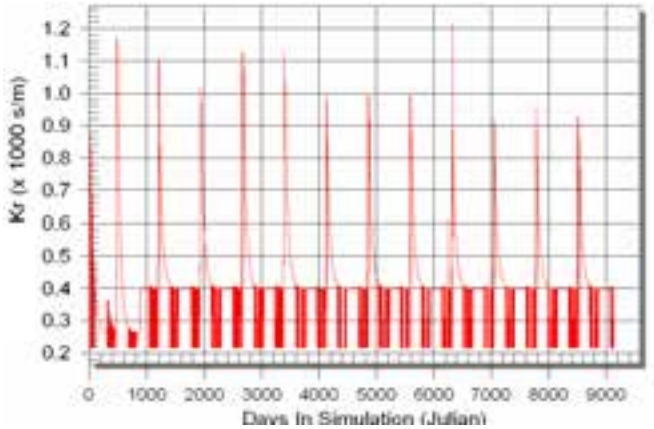

Figure 11b – Rill erodibility

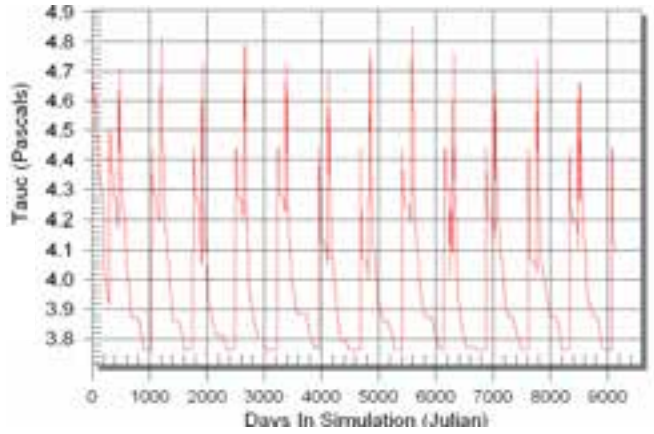

Figure 11c – Critical fluvial erosional strength

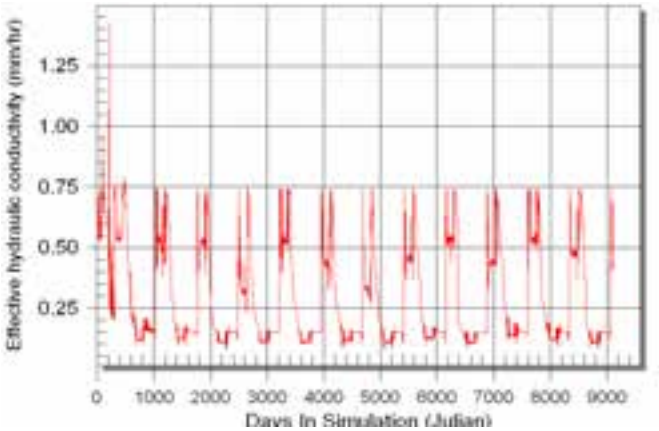

Figure 11d – Effective hydraulic conductivity

The scaled maps shown in Figures 12a, 12b provide the runoff volume in cubic meters per year for the 113 hillslopes.

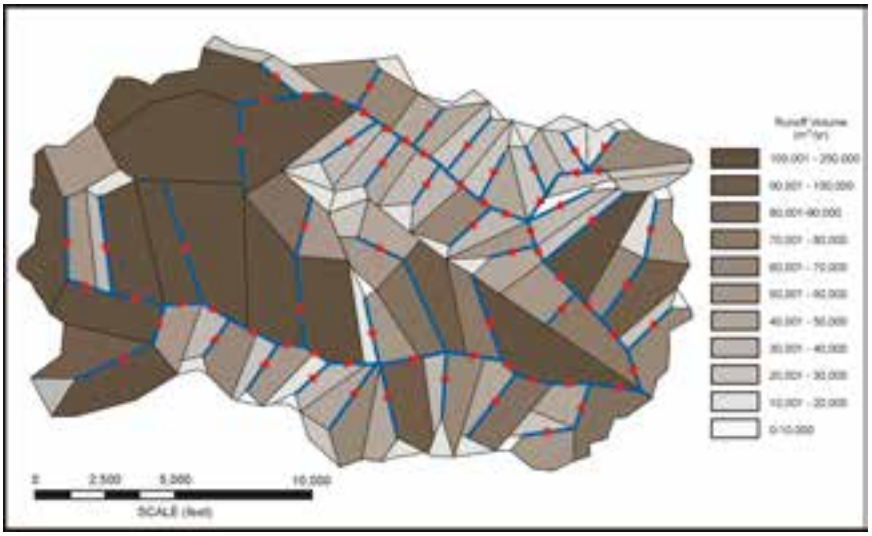

Figure 12a – Runoff volume (m^3/yr) for 25 years WEPP simulation

Please note that similar figures have been generated for all continuous simulations; however, the 25 year simulation is presented here in a great detail since this case corresponds to the commencement period for the equilibrium conditions.

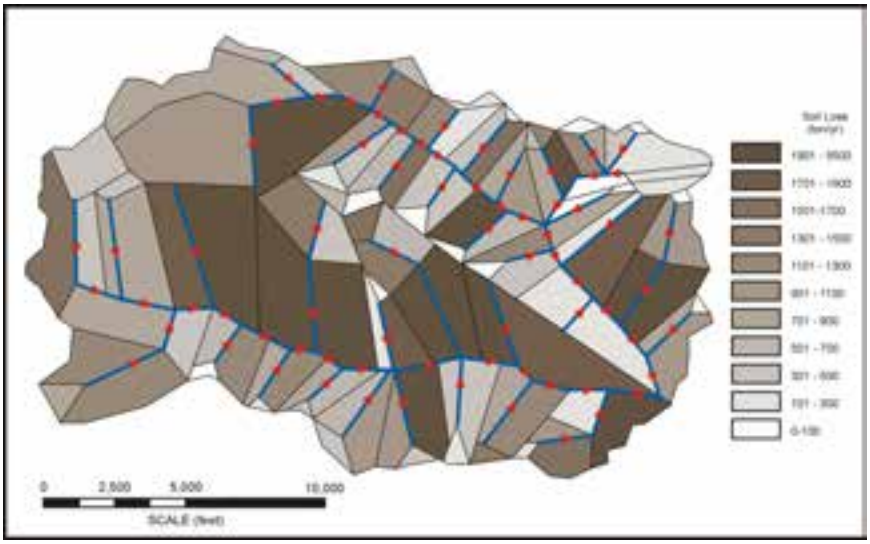

Figure 12b – Soil loss (ton/yr) for 25 years WEPP simulation

The SDR based on the 25-year continuous simulation is 0.183. This means that 18.3% of the total eroded sediment reaches the watershed outlet. The runoff and soil loss shown in figures 12a and 12b are absolute quantities. These maps were constructed for the 25 year simulation. The 25 year simulations were compared with historic measurements obtained by the USGS during the period of 1952-2005. Figures 13a and 13b demonstrate the USGS monthly stream flow and precipitation variations.

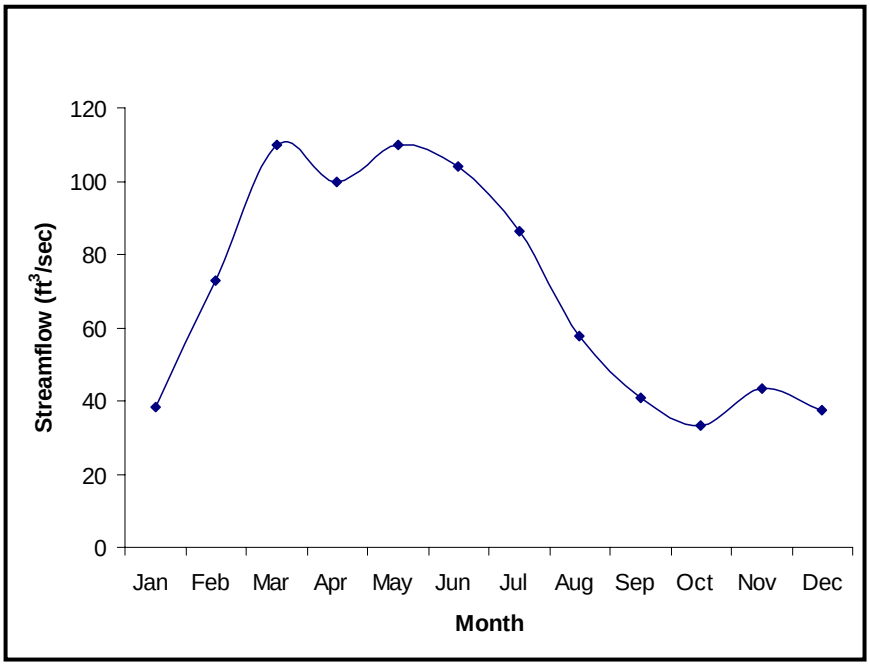

Figure 13a – Monthly streamflow variation for USGS stream-gage at Clear Creek near Coralville, IA for periods (1952–2005)

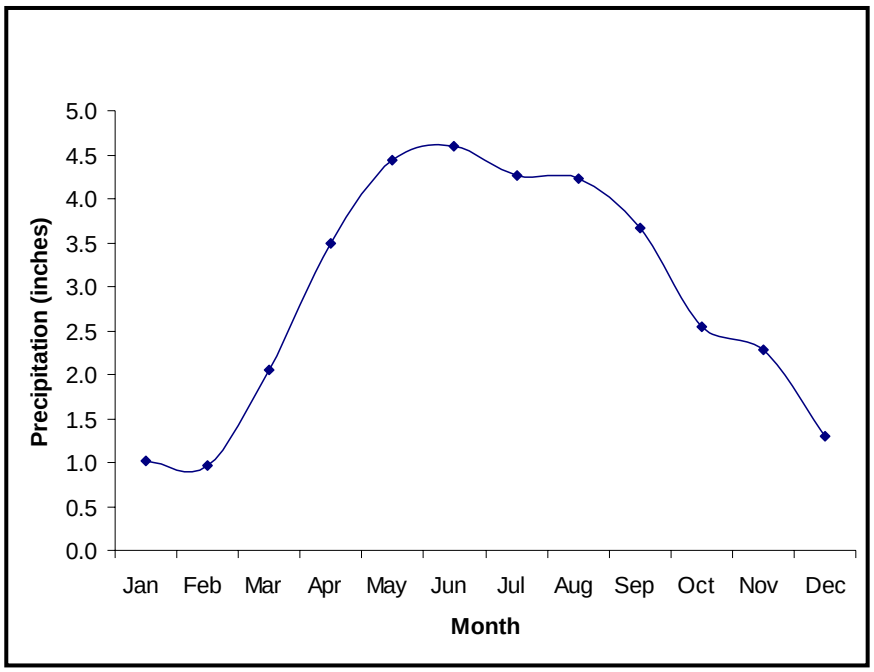

Figure 13b – Monthly precipitation for the Williamsburg, IA station for periods (1952–2005)

Figure 13c provides the reconstructed relation between suspended sediment and flow discharge. As expected the relation between sediment and flow is described by a power law.

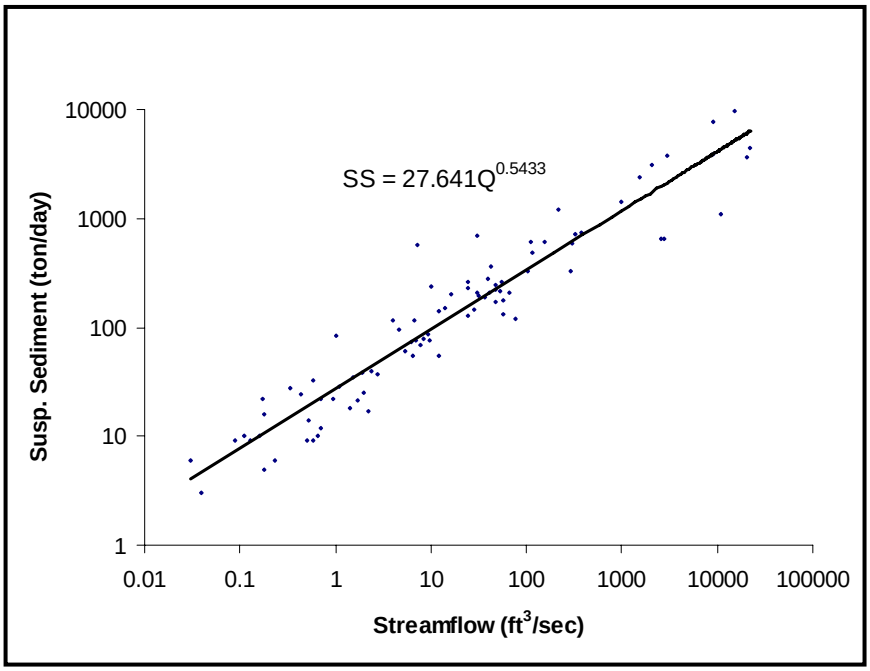

Figure 13c – Suspended sediment – streamflow relation for USGS streamgage Clear Creek near Coralville, IA for periods (1964 – 1973)

An interpolation technique was used to transfer these data from the Coralville site to the Oxford site. The interpolation was based on the consideration that the drainage area is

proportional to the flow at the Coralville site. Specifically it was determined based on the data that the flow at the outlet of the South Amana catchment was about 10 times smaller than the flow in Coralville stream gauge. Using the flow ratio and the suspended sediment-flow relation, it was determined that during the peak months of March, April, May and June an averaged erosion rate of 100 tons/day occurs. In the remaining 8 months the average rate is close to 35 tons/day. The weighted average of these rates provides the annual averaged sediment yield at the outlet of the South Amana area which is about 21,000 tons/year. This is very close to the estimated 26,334 tons/year sediment discharge.

Table 16 summarizes the SDR values for the continuous simulations. It shows that SDR reaches an equilibrium value at about 100 years. This table indicates that on average 13% of the eroded sediment reaches into the watershed outlet. This finding may have implications for setting EPA standards/limits for nutrients and sediments.

Table 16 – Continuous simulations SDR results

Period	SDR	Period	SDR
(yrs)	(---)	(yrs)	(---)
2	0.363	25	0.183
5	0.158	50	0.143
10	0.231	100	0.125
15	0.190	150	0.121
17	0.195	200	0.133
20	0.201		

Figure 13d complements the findings of Table 17.

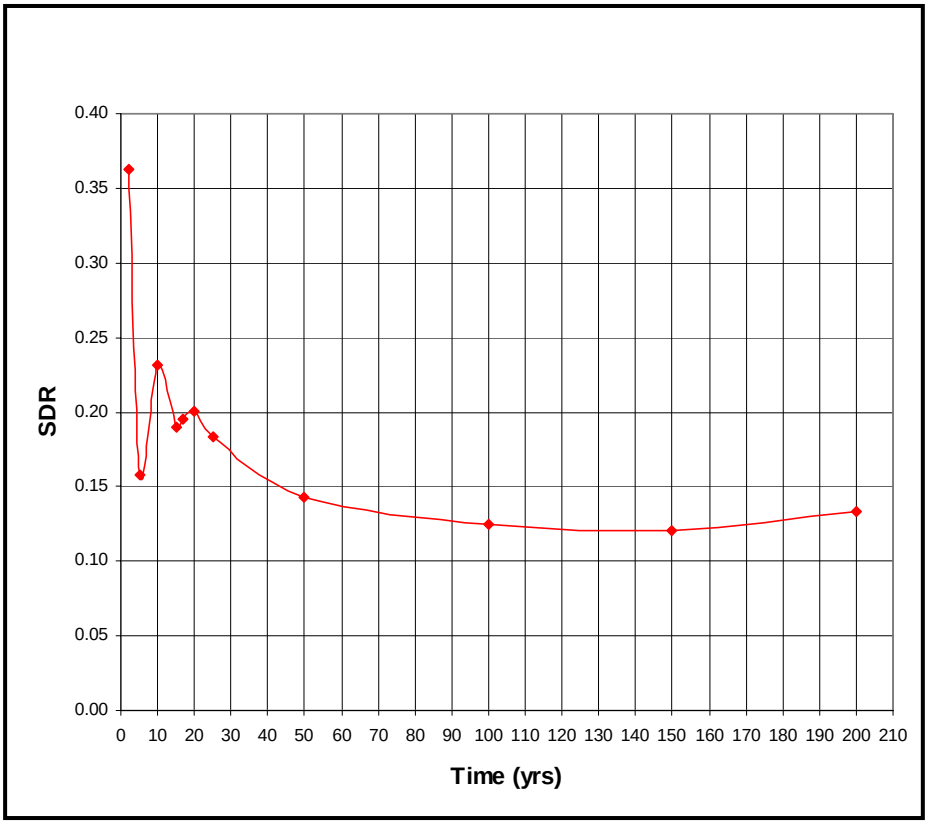

Figure 13d – Sediment Delivery Ratio

An average annual soil loss estimate of 20.3 ton/ha/yr is calculated via RUSLE2. WEPP estimate for the same quantity is 53.1 ton/ha/yr. It is shown that the WEPP estimate of soil loss for the 25 years simulation is approximately 2.5 times larger than the RUSLE2 estimate. This discrepancy is attributed to the fact that WEPP can adequately simulate the detachment and deposition processes occurring in the hillslopes while RUSLE2 cannot.

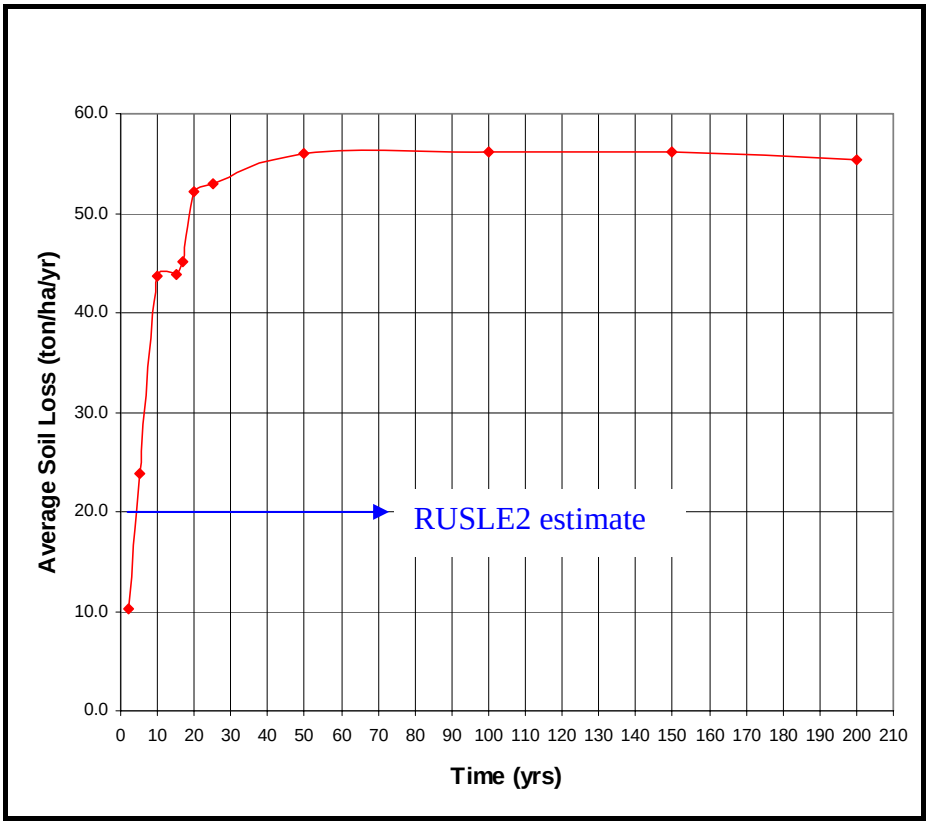

Figure 13e – Average soil loss in case of continuous simulations

4.2 Event Simulation:

The results of the event simulations are important for performing pollution predictions and comparisons with field measurements. Since continuous simulations are averaged yearly, they cannot provide a direct comparison between measured and estimated pollutant transport. The storm of 6/25/06 was determined to be the strongest storm in 2005. Table 9 summarizes the duration characteristics of the June 25th 2005 storm. First, WEPP was run for the 113 hillslopes to determine the volumetric discharges as 75,8024 m^3. The corresponding sediment discharge at the outlet is 3143.2 tons/year, and the annual sediment yield per unit hectare is 4.5 tons/ha. The sediment delivery ratio for the single storm is 0.656, almost three times higher than the reported SDR value for the 25 year continuous simulation. (See Table 17) This implies that pollutant predictions that are based on continuous simulations may not be appropriate, even if these continuous simulations correspond to equilibrium conditions. In the single storm case 65.6% of the soil ends up into the Clear Creek watershed. Based on the Brune's delivery curves, 100% of the eroded material ends up into the Creek and eventually to the catchment outlet. If there is some discrepancy between the WEPP predictions and the Brune's delivery curves this has to do with the steady nature of the Brune's method. Here it is notable that despite their limitations

both WEPP and Brune's delivery methods are overall in agreement. Figures 14a and 14b present the runoff volume in m^3 and the soil loss in tons for the 06/25/05 storm simulation. The single storm event simulations are useful for isolating the areas that are prone to erosion. Such information is useful in identifying the plots within the watershed that require BMPs.

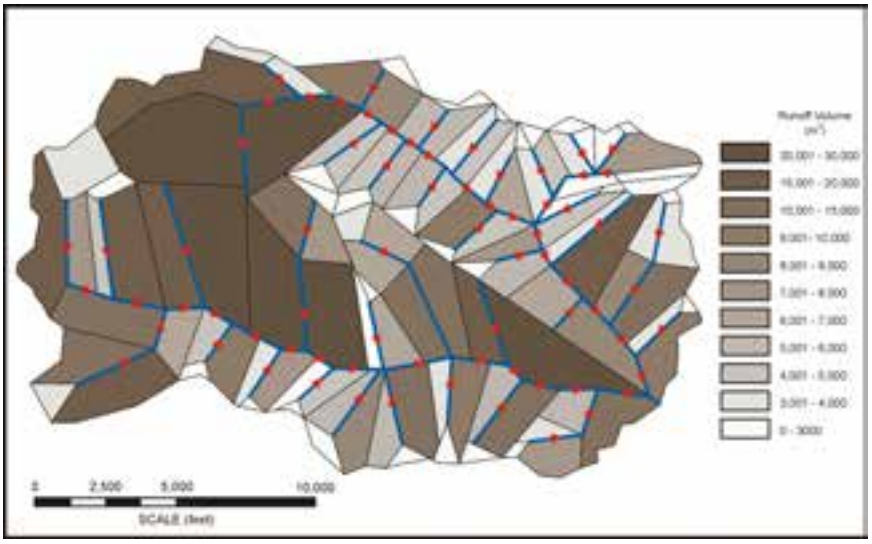

Figure 14a – Runoff volume (m^3) for WEPP simulation of 06/25/05 storm

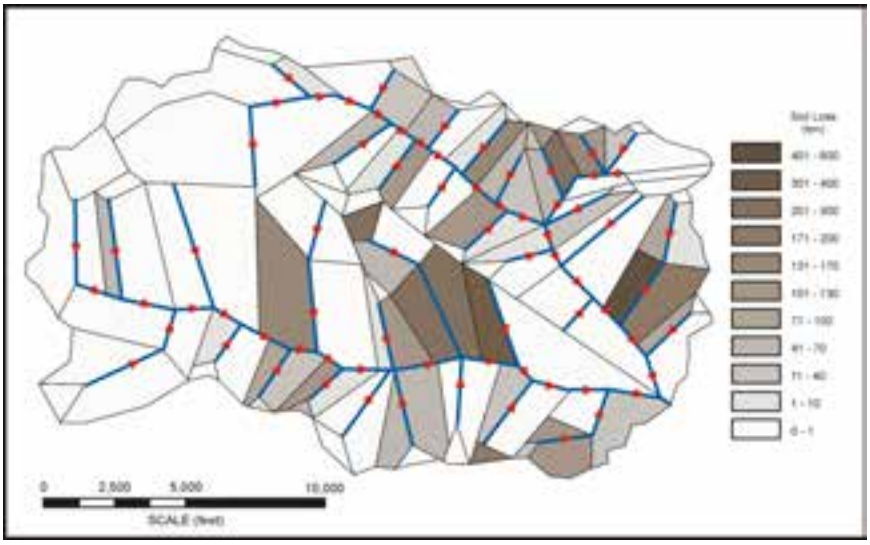

Figure 14b – Soil loss (ton) for WEPP simulation of 06/25/05 storm

The erosion and runoff WEPP results are incorporated into the phosphorus modulus to determine total amount of phosphorus that is transported during 06/25/05 storm event. Those estimations were based on the consideration that this event is the one that affects the water quality in the Clear Creek since most of the sediment reaches into the stream. This

assumption appears to be sound but requires further testing, by performing future research such as continuous and/or storm event monitoring. The theoretical equations used for determining the dissolved and undissolved phase of phosphorus have been described in the methodology chapter.

Table 17 summarizes the parameters used in the phosphorus load calculations.

Table 17 –Parameters used in phosphorus load calculations

Parameter	Value
CPKD	1.75
β	0.44
Bray P (µg/g)	35.0
CPLAB (µg/g)	9.10
ER	1.67

Table 18 summarizes the total phosphorus runs for the 6/25/05 event.

Table 18 –Phosphorus loads for each hillslope

HillSlopes	Sediment Yield (kg/ha)	Runoff Depth (cm)	C (mg/g)	CPLABW (mg/l)	ROLP (kg/ha)	ROLP (mg/l)	SEDLP (kg/ha)
H1	0.00	4.04	0.57	0.14	0.06	0.14	0.00
H2	841.53	4.16	0.63	0.16	0.06	0.16	38.21
H3	17764.89	4.60	0.91	0.23	0.10	0.23	1168.72
H4	6039.50	4.24	0.67	0.17	0.07	0.17	294.78
H5	3769.28	4.23	0.66	0.16	0.07	0.16	181.44
H6	856.38	4.26	0.68	0.17	0.07	0.17	42.20
H7	0.00	4.13	0.61	0.15	0.06	0.15	0.00
H8	29967.62	4.31	0.71	0.18	0.08	0.18	1543.61
H9	0.00	4.23	0.66	0.16	0.07	0.16	0.00
H10	0.00	4.05	0.57	0.14	0.06	0.14	0.00
H11	0.00	2.98	0.27	0.07	0.02	0.07	0.00
H12	4339.73	4.32	0.71	0.18	0.08	0.18	224.60
H13	1934.23	4.19	0.64	0.16	0.07	0.16	90.34
H14	98.90	4.14	0.62	0.15	0.06	0.15	4.44
H15	16.58	4.23	0.66	0.16	0.07	0.16	0.80
H16	8.52	4.18	0.64	0.16	0.07	0.16	0.39
H17	0.00	3.10	0.29	0.07	0.02	0.07	0.00
H18	24000.40	4.80	1.07	0.27	0.13	0.27	1870.96
H19	207.80	4.21	0.65	0.16	0.07	0.16	9.85
H20	22599.06	4.43	0.78	0.19	0.09	0.19	1285.89
H21	13854.97	4.56	0.87	0.22	0.10	0.22	878.29
H22	1416.96	4.21	0.65	0.16	0.07	0.16	67.16
H23	574.84	4.22	0.66	0.16	0.07	0.16	27.42
H24	424.27	4.20	0.65	0.16	0.07	0.16	20.01
H25	0.00	4.13	0.61	0.15	0.06	0.15	0.00
H26	0.00	4.07	0.58	0.14	0.06	0.14	0.00
H27	0.00	2.76	0.24	0.06	0.02	0.06	0.00
H28	0.00	3.36	0.34	0.09	0.03	0.09	0.00
H29	0.00	4.11	0.60	0.15	0.06	0.15	0.00
H30	0.00	4.08	0.59	0.15	0.06	0.15	0.00
H31	0.00	2.72	0.23	0.06	0.02	0.06	0.00
H32	0.00	4.14	0.62	0.15	0.06	0.15	0.00
H33	0.00	4.10	0.60	0.15	0.06	0.15	0.00

Table 18 –Phosphorus loads for each hillslope (continued)

HillSlopes	Sediment Yield (kg/ha)	Runoff Depth (cm)	C (mg/g)	CPLABW (mg/l)	ROLP (kg/ha)	ROLP (mg/l)	SEDLP (kg/ha)
H34	0.00	0.85	0.20	0.05	0.00	0.05	0.00
H35	0.00	3.30	0.33	0.08	0.03	0.08	0.00
H36	4914.44	4.49	0.83	0.21	0.09	0.21	294.77
H37	0.00	3.17	0.30	0.08	0.02	0.08	0.00
H38	0.00	3.24	0.32	0.08	0.03	0.08	0.00
H39	0.00	4.14	0.62	0.15	0.06	0.15	0.00
H40	12.76	3.42	0.36	0.09	0.03	0.09	0.33
H41	2407.20	4.17	0.63	0.16	0.07	0.16	110.27
H42	0.00	4.11	0.60	0.15	0.06	0.15	0.00
H43	0.00	4.11	0.60	0.15	0.06	0.15	0.00
H44	0.00	3.37	0.35	0.09	0.03	0.09	0.00
H45	8260.99	4.33	0.72	0.18	0.08	0.18	433.91
H46	1562.99	4.56	0.87	0.22	0.10	0.22	98.98
H47	0.00	4.02	0.56	0.14	0.06	0.14	0.00
H48	9596.35	4.29	0.70	0.17	0.07	0.17	486.82
H49	9778.69	4.31	0.71	0.18	0.08	0.18	503.38
H50	0.00	4.12	0.61	0.15	0.06	0.15	0.00
H51	3061.13	4.22	0.66	0.16	0.07	0.16	146.47
H52	836.79	3.03	0.28	0.07	0.02	0.07	16.88
H53	0.00	3.02	0.28	0.07	0.02	0.07	0.00
H54	15734.68	4.38	0.75	0.19	0.08	0.19	855.55
H55	0.00	3.06	0.28	0.07	0.02	0.07	0.00
H56	0.00	4.15	0.62	0.15	0.06	0.15	0.00
H57	13173.44	4.57	0.88	0.22	0.10	0.22	845.03
H58	0.00	4.09	0.59	0.15	0.06	0.15	0.00
H59	5957.88	4.22	0.66	0.16	0.07	0.16	285.13
H60	31022.65	4.53	0.85	0.21	0.10	0.21	1919.11
H61	456.54	4.20	0.65	0.16	0.07	0.16	21.54
H62	9032.68	4.43	0.78	0.19	0.09	0.19	513.35
H63	0.00	4.12	0.61	0.15	0.06	0.15	0.00
H64	0.00	4.13	0.61	0.15	0.06	0.15	0.00
H65	33.55	4.37	0.75	0.19	0.08	0.19	1.82
H66	0.00	2.64	0.22	0.06	0.01	0.06	0.00
H67	2052.56	4.29	0.70	0.17	0.07	0.17	103.64
H68	0.00	4.43	0.78	0.19	0.09	0.19	0.00
H69	0.00	4.10	0.60	0.15	0.06	0.15	0.00
H70	0.00	2.64	0.22	0.05	0.01	0.05	0.00
H71	0.00	3.16	0.30	0.07	0.02	0.07	0.00
H72	24216.10	4.54	0.86	0.21	0.10	0.21	1507.08
H73	5028.85	4.34	0.73	0.18	0.08	0.18	265.50
H74	20404.64	4.27	0.68	0.17	0.07	0.17	1015.15
H75	21165.99	4.76	1.04	0.26	0.12	0.26	1598.61
H76	25359.97	4.70	0.98	0.24	0.11	0.24	1808.32
H77	0.00	4.06	0.58	0.14	0.06	0.14	0.00
H78	0.00	3.16	0.30	0.08	0.02	0.08	0.00
H79	9141.73	4.61	0.91	0.23	0.10	0.23	606.09
H80	0.00	4.06	0.58	0.14	0.06	0.14	0.00

Table 18 –Phosphorus loads for each hillslope (continued)

HillSlopes	Sediment Yield (kg/ha)	Runoff Depth (cm)	C (mg/g)	CPLABW (mg/l)	ROLP (kg/ha)	ROLP (mg/l)	SEDLP (kg/ha)
H81	1373.83	4.21	0.65	0.16	0.07	0.16	65.14
H82	7434.85	4.38	0.75	0.19	0.08	0.19	405.95
H83	5150.53	4.19	0.64	0.16	0.07	0.16	240.75
H84	15866.08	4.53	0.85	0.21	0.10	0.21	982.32
H85	773.44	4.31	0.71	0.18	0.08	0.18	39.82
H86	0.00	4.20	0.65	0.16	0.07	0.16	0.00
H87	0.00	4.08	0.59	0.15	0.06	0.15	0.00
H88	4959.44	4.27	0.69	0.17	0.07	0.17	246.86
H89	0.00	4.11	0.60	0.15	0.06	0.15	0.00
H90	597.31	4.17	0.63	0.16	0.07	0.16	27.36
H91	0.00	4.12	0.61	0.15	0.06	0.15	0.00
H92	1081.21	3.46	0.37	0.09	0.03	0.09	28.91
H93	855.70	4.28	0.69	0.17	0.07	0.17	42.82
H94	0.00	2.26	0.19	0.05	0.01	0.05	0.00
H95	0.00	3.05	0.28	0.07	0.02	0.07	0.00
H96	0.00	2.30	0.19	0.05	0.01	0.05	0.00
H97	0.00	3.04	0.28	0.07	0.02	0.07	0.00
H98	6026.50	4.36	0.74	0.18	0.08	0.18	324.54
H99	0.00	4.20	0.65	0.16	0.07	0.16	0.00
H100	0.00	2.98	0.27	0.07	0.02	0.07	0.00
H101	869.84	4.26	0.68	0.17	0.07	0.17	42.88
H102	10182.61	4.36	0.74	0.18	0.08	0.18	547.81
H103	0.00	2.40	0.20	0.05	0.01	0.05	0.00
H104	0.00	4.10	0.60	0.15	0.06	0.15	0.00
H105	0.00	4.12	0.61	0.15	0.06	0.15	0.00
H106	0.00	1.46	0.16	0.04	0.01	0.04	0.00
H107	4454.32	4.21	0.66	0.16	0.07	0.16	212.16
H108	179.06	4.23	0.66	0.16	0.07	0.16	8.61
H109	0.00	3.13	0.30	0.07	0.02	0.07	0.00
H110	418.45	4.17	0.63	0.16	0.07	0.16	19.26
H111	0.00	4.09	0.59	0.15	0.06	0.15	0.00
H112	0.00	2.99	0.27	0.07	0.02	0.07	0.00
H113	0.00	2.23	0.18	0.05	0.01	0.05	0.00

The averaged P that is attached to sediments is 122.64 kg/ha and the concentration of the dissolved phase is 0.123 mg/l. The amount of orthophosphate compares favorably with the samples obtained through the IOWATER project. The orthophosphate amount measured was 0.2 mg/l.

5. CONCLUSIONS

1. WEPP compares well with direct measurements for continuous and single storm simulations. This is not coincidental considering that the model has been calibrated, verified and is based on sound physics. On the contrary, the lumped model RUSLE2 overestimates erosion since it does not have inherently the ability to simulate the flow and soil delivery pathways correctly. RUSLE2 does not differentiate between convex and concave hillslopes and their effects on flow and sediment pathways.

2. WEPP is user friendly and proves to be easier to use than RUSLE2. The built-in databases provide to the user different alternatives, a capability that is not fully available at RUSLE2. At RUSLE2 you do not have the capability to modify or save certain input files, i.e. modification of soils input is not allowed and land use timeline can not be saved after making modifications.

3. The continuous simulations reveal that in order for the Clear Creek watershed to reach equilibrium conditions at least 50 years need to be passed for the fluid phase and at least 100 years for the solid phase. This has significant implications for NPS control. It suggests that for nutrient loads found in dissolved phase at least 50 years need to be passed for the system to regain its prior condition. For sediments and P, 100 hundred years are required.

4. The travel time for sediment delivery increases as the period of continuous simulations increases. This is shown clearly with the reduction of the SDR as the simulation period increases. About 10% of the total eroded material reaches the watershed outlet at equilibrium conditions.

5. Equilibrium conditions can be used to set the limits for P and other nutrients. Equilibrium conditions clearly provide the controlling time scales for the solid and dissolved phases.

6. The strong event, single storm simulation shows that 65.6% of the material ends up into the stream. This has some practical implications with respect to BMPs for isolating and controlling the areas that contribute the most to sediment and P. It suggests the following:

a) The number and magnitude of these storms throughout a year is necessary to be determined

b) The probability of occurrence of these storms needs to be determined

c) The areas contributing to erosion the most need to be identified and controlled with BMPs

d) The application of fertilizers should not be taken place at the period of occurrence of these strong storms.

7. Future research should focus on the symbiotic relationship between models and sensors. Dynamic modeling allows accurate prediction and can become an important tool for TMDLs.

8. TMDLs need to be technically sound and founded on models.

6. REFERENCES

Foster GR, Flanagan DC, Nearing MA, Lane LJ, Risse LM and Finkner SC (1995) Chapter 11: Hillslope Erosion Component In USDA Water Erosion Prediction Project Hillslope Profile and Watershed Model Documentation, Vol. NSERL Report No. 10 Eds, Flanagan, D. C. and M. A. Nearing. USDA-ARS national Soil Erosion Research Laboratory.

Klatt, J. G., Mallarino, A. P., Downing, J. A., Kopaska J. A., Wittry D. J. 2003. Soil phosphorus, management practices, and their relationship to phosphorus delivery in the Iowa Clear Lake agricultural watershed. J Environ Qual, 32: 2140-2149.

Leonard, R. A., W. G. Knisel, and D. A. Still. 1987. GLEAMS: Groundwater Loading Effects of Agricultural Management Systems. Transactions of the American Society of Agricultural Engineers, 30(5):1403-1418.

Sharpley, A. N., C. A. Jones, C. Gray, and C. V. Cole. 1984. A simplified soil and plant phosphorus model: II. Prediction of labile, organic, and absorbed phosphorus. J. Soil Sci. Soc. Am. 48(4): 805–809.

Stone, J.J., L.J. Lane and E.D. Shirley. 1992. Infiltration and runoff simulation on a plane. Transactions of the ASAE 35(1):161-170.